

THE PENNSYLVANIA STATE UNIVERSITY
SCHREYER HONORS COLLEGE

DEPARTMENT OF ELECTRICAL ENGINEERING

QUANTITATIVE ANALYSIS OF THE HUMAN AIRWAY TREE USING HIGH
RESOLUTION MDCT DATA

MICHAEL AMTHOR
SPRING 2013

A thesis
submitted in partial fulfillment
of the requirements
for a baccalaureate degree
in Electrical Engineering
with honors in Electrical Engineering

Reviewed and approved* by the following:

William Higgins
Distinguished Professor of Electrical Engineering
Thesis Supervisor
Honors Adviser

Jeffrey Mayer
Associate Professor of Electrical Engineering
Faculty Reader

* Signatures are on file in the Schreyer Honors College.

ABSTRACT

The Multidimensional Image Processing Lab (MIPL) at the Pennsylvania State University has developed a software suite designed to aid in navigational bronchoscopy. The MIPL suite takes a high-resolution computed tomography (CT) patient chest scan and creates a 3D reconstruction of the patient's chest anatomy. Associated with this process is the generation of a quantitative representation of the airway tree, extracted via image processing techniques developed by the MIPL. Quantitative measurement is possible due to the known dimensions and orientation of chest CT scans. Current methods and the MIPL's work in planning navigational bronchoscopies have led to an unprecedented availability of high-resolution 3D data. Because of the exhaustive verification of the MIPL suite's efficacy, we take interest in using the data produced by the MIPL in a quantitative analysis of the human airway tree. The data utilized in this analysis come from 81 patient chest scans accrued over the years by the MIPL. Each case must first be individually processed by the MIPL suite and then by a C++ program we have designed to create a standardized output file. The output files of many cases are then compiled and further processed by a MATLAB program designed to calculate aggregate statistics. Finally, these statistics are organized into plots and tables to give a statistical representation of the airway tree. We observe branch diameters, lengths, and angles by generation, lobar generation and lobe for the entire population, and compare branch measurements between genders and among body mass index classifications. We note a decrease in branch size with an increase in generation, supported by Ewald Weibel's conclusions. We also observe a larger branch size in males than in females, and an increase in branch diameters with BMI except in obese patients.

TABLE OF CONTENTS

List of Figures.....	iii
List of Tables.....	vi
Acknowledgements.....	vii
Chapter 1 Introduction	1
Chapter 2 Anatomy of the Human Lung.....	5
2.1: Top-Level Lung Anatomy	5
2.2: Branch Representation.....	6
2.3: Branching Pattern	7
Chapter 3 Methods.....	12
3.1: MIPL Preprocessing	14
3.2: Completion of Single-Case Analysis.....	16
3.2.1: Key Branch Identification.....	17
3.2.2: Writing the Output File	21
3.3: Multi-Case Analysis	24
3.3.1: Creating the Analysis File	26
3.3.2: Generating Plots and Tables	32
Chapter 4 Data and Results	33
4.1: Database.....	33
4.2: Results.....	37
4.2.1: Global Analysis.....	39
4.2.2: Analysis by Gender.....	57
4.2.3: Analysis by BMI.....	58
Chapter 5 Discussion and Future Work	60
5.1: Conclusions	60
5.2: Future Directions	60
Appendix A Cases Used	62
Appendix B User Manual	88
BranchStats.....	88
MATLAB.....	89
BIBLIOGRAPHY	92

LIST OF FIGURES

Figure 1.1: Volume representation by individual slices. (a) A single slice. (b) Multiple slices representing the chest volume.	3
Figure 2.1: Lobes (and lingula) of the human lung. (a) Lobes are separated to show relative size and shape. (b) Lobes are connected as in normal anatomy to show full lung structure.....	6
Figure 2.2: Illustration of a single branch (shaded) as it connects to its proximal parent and distal daughter branches.	7
Figure 2.3: Branching pattern of the trachea (generation 0), main bronchi (generation 1), five lobar parents, right intermediary bronchus, and lingula parent. The dotted ovals represent the rough outlines of the right and left lungs.	9
Figure 2.4: Branching pattern illustrated in the 3D rendering of patient 20349_3_55. (a) The entire tree is shown. (b) The airways of the hilum are expanded and key branches identified.	10
Figure 3.1: Flow chart showing single case analysis. The input is an image file and the output is a BranchData text file. The .npth file is created as an intermediate and serves as the input to BranchStats.	12
Figure 3.2: Flow chart showing multi-case analysis. The input is a directory folder of BranchData text files and the output is in the form of Excel graphs and tables. The Analysis file is generated as an intermediate.	13
Figure 3.3: Process of creating a BranchData file using an .npth file as input.	16
Figure 3.4: Multi-case analysis process.	25
Figure 3.5: Snapshot of a single Analysis file. Branches are grouped by the entire tree, by lobe, by generation, by lobar generation. Left main bronchus and right main bronchus statistics are also displayed in the file.....	31
Figure 4.1: 3D rendering of airway tree for case 20349_3_62. The tree contains 223 branches. Processing completed using B31 and B50 images.....	34
Figure 4.2: Sample data in .npth file. The file displays total number of branches in the case, as well as parent branch ID for each branch and the position of all viewsites in the branch. These are the data of importance in Section 3.2. This .npth file corresponds to the tree in Figure 4.1 (20349_3_62).....	35
Figure 4.3: Abnormal right middle and lower lobe branching pattern observed in several cases. Branch 1 is the right middle lobe parent, by inspection of interlobar fissures. Branches 2 and 4, however, are both within the right lower lobe. In the BranchData file, branch 2 is designated the right lower lobe parent and branch 1 is designated the right middle lobe parent. Branches 2, 3, 4, and all daughters of branches 2 and 4 are	

labeled right lower lobe branches, while all daughters of branch 1 are labeled right middle lobe branches.	36
Figure 4.4: Abnormal geometry explained in Figure 4.3. (a) The entire airway tree, rotated to show the right lower and middle lobes. (b) Expanded view of right intermediary bronchus and children in abnormal pattern. The branch numbers used in Figure 4.4 correspond to those used in Figure 4.3.....	37
Figure 4.5: Average branch diameter vs. generation number for the entire population up to generation 13. The x-axis values represent the generation number. The number in parentheses represents the number of cases represented by that generation. Endpoints of the bars represent 5 th and 95 th percentiles. Note the y-axis is a logarithmic scale with base 2.	40
Figure 4.6: Comparison between the average diameter data generated by our study (black) and Weibel's calculations for an airway tree exhibiting a normal dichotomy (gray) [1]. Note the base 2 logarithmic scale.	42
Figure 4.7: Average branch diameter vs. lobar generation number for the entire population up to lobar generation 11. The x-axis values represent the lobar generation number. The number in parentheses represents the number of cases with branches in that generation. Bars represent 5 th and 95 th percentiles.	44
Figure 4.8: Average branch diameter vs. generation number for the entire population up to generation 13 excluding the trachea. The trachea's starting point is arbitrarily defined in the MIPL software, rendering length data unreliable. The x-axis values represent the generation number. The number in parentheses represents the number of cases represented by that generation. Bars represent 5 th and 95 th percentiles. Note the y axis is a base 2 logarithmic scale.	46
Figure 4.9: Comparison between branch length the data generated by our study (black) and Weibel's calculations (gray) [1]. Note the base 2 logarithmic scale.	48
Figure 4.10: Branch length vs. lobar generation number for the entire population up to lobar generation 11. The x-axis values represent the lobar generation number. The number in parentheses represents the number of cases with branches in that lobar generation. Bars represent 5 th and 95 th percentiles.	49
Figure 4.11: Mean angle with parent branch vs. generation number. Note only data up to generation 13 is displayed in the plot.	51
Figure 4.12: Angle with parent vs. lobar generation number. Note only up to lobar generation 11 is displayed in the plot.	53
Figure 4.13: (a) Illustration of extreme (near 180° or 0) branch angles. Angle vector axes (AVAs, dashed lines) are extensions of vectors made from distal three (parent) or proximal three (daughter) viewsites. The angle between the parent AVA and daughter 1 AVA is near 180° while the angle between the parent AVA and daughter	

1 AVA is near 0. (b) Extreme angle in case 21405_12. Branch 279 (centerline in blue) leaves at approximately 175°.....	55
Figure 4.14: Average branch diameters by lobe. Columns represent the mean diameters. Bars represent the 5 th and 95 th percentiles. Note each lobe contains a range of generations, contributing to the large range of diameters in each lobe.....	56
Figure 4.15: Mean average branch diameter vs. lobar generation for both males and females. The numbers in parentheses represent the number of cases containing branches in that generation for each gender (male, female). Note the base 2 logarithmic y-axis scale.	57
Figure 4.16: Mean branch length vs. lobar generation for both males and females. The numbers in parentheses represent the number of cases containing branches in that generation for each gender (male, female). Note the base 2 logarithmic y-axis scale.....	58
Figure 4.17: Average branch diameter vs. lobar generation number for all four BMI classifications. Note the base 2 logarithmic y-axis scale.....	59

LIST OF TABLES

Table 4.1: Statistics for average branch diameter by generation for all generations. Right and left main bronchus data is listed separately beneath generation 1 data. Ewald Weibel's mean diameter findings are listed in the last column [1]. All measurements are in mm.	41
Table 4.2: Statistics for average branch diameter by lobar generation for all lobar generations. All measurements are in mm.	45
Table 4.3: Statistics for branch length by generation for all generations. Right and left main bronchus data is listed separately beneath generation 1 data. Ewald Weibel's mean branch length calculations are listed in the last column [1]. All measurements are in mm.	47
Table 4.4: Statistics for branch length by lobar generation for all lobar generations. All measurements are in mm.	50
Table 4.5: Table of angle with parent statistics by generation for all cases.	52
Table 4.6: Table of angle with parent statistics by lobar generation.....	54
Table A.1: Cases used in our study.....	66
Table A.2: 3D renderings of all cases used in the study. Each rendering has protocol number, gender, BMI classification, and notes corresponding to Table A.1 listed in that order underneath. M=male, F=female, U=underweight, N=normal weight, Ov=overweight, Ob=obese, and N/A=unknown.	87

ACKNOWLEDGEMENTS

This work was partially supported by NIH grant R01-CA151433 from the National Cancer Institute. Data was drawn from Penn State Hershey Medical Center IRB protocols 20349 and 21405.

I would like to take this opportunity to thank Dr. William Higgins and Dr. Rebecca Bascom, as well as Dr. Duane Cornish, Dr. Rahul Khare, Ronnarit Chiersilp, Xiaonan Zang, Patrick Byrnes, and the multitude of personnel at Penn State Hershey Medical Center for helping guide this project to completion.

I would also like to thank my parents, Nancy and Phil, as well as Brittany Davis, for all of their support throughout the process.

Chapter 1

Introduction

The Multidimensional Image Processing Lab (MIPL) at Penn State has accrued a wealth of quantitative airway tree data through research in navigational bronchoscopy. In our study, we have developed methods to extract and orient data of interest into a series of plots and tables to give a quantitative overview of the human airway tree. This allows us to view trends within the airway tree, and to view anatomical similarities and differences among subgroups of patients.

Throughout the course of medicine, there has been much inquiry into both the structure and the function of the human lung. Several studies have been performed to investigate these properties both qualitatively and quantitatively, but the extent of any study is limited by the technology of its time. Ewald Weibel's 1963 book, "Morphometry of the Human Lung," outlined an analysis based on the use of preserved, deceased tissue combined with bronchograms, though these samples are certainly not numerous and are tedious to obtain [1]. In the second half of the 20th century and into the 21st century, drastic advances in medical imaging have produced ever more accurate and precise measurements of the dimensions of the human lung. The advent of the single-row computed tomography (CT) scan followed by multi-detector CT (MDCT) scanners has allowed us to view a slice representation of the volume of the human chest from many different axes and to reconstruct this data into a three-dimensional (3D) rendering of the airway tree [3]. This has led to further study into the geometry and structure of the human airway [4, 5], as well the development of software for clinical applications [6, 7].

The MIPL has developed a software suite for virtual bronchoscopy which uses high resolution MDCT data as input [6, 10, 11, 12]. This software suite constructs a 3D rendering of

the airway tree along with a text representation of airway statistics, called the .npth file. Over the past several years, the MIPL has accrued a number of MDCT chest scans through several navigational bronchoscopy studies. However, a global quantitative analysis of the human airway tree has not been performed using this data. Such an analysis may help improve current techniques in navigational bronchoscopy, such as route planning and choice of devices [12, 13]. We have developed two software programs designed to give an aggregate statistical view (both graphical and tabular) of cases accrued by the MIPL using the .npth files from these cases.

Because of the obvious difficulties of directly observing the anatomy of a vital organ in the body cavity of a living specimen, many methods have been devised for producing images of internal structure. Of particular interest when considering the soft tissue in the lung and mediastinum is X-ray computed tomography (CT) scanning. Unlike the previously used simple analog X-ray images, which show superposition images of complete body sections, CT allowed for the view of discrete planes within the section under observation, with the planes aggregating to allow for “volume representation by single slices,” shown in Figure 1.1.

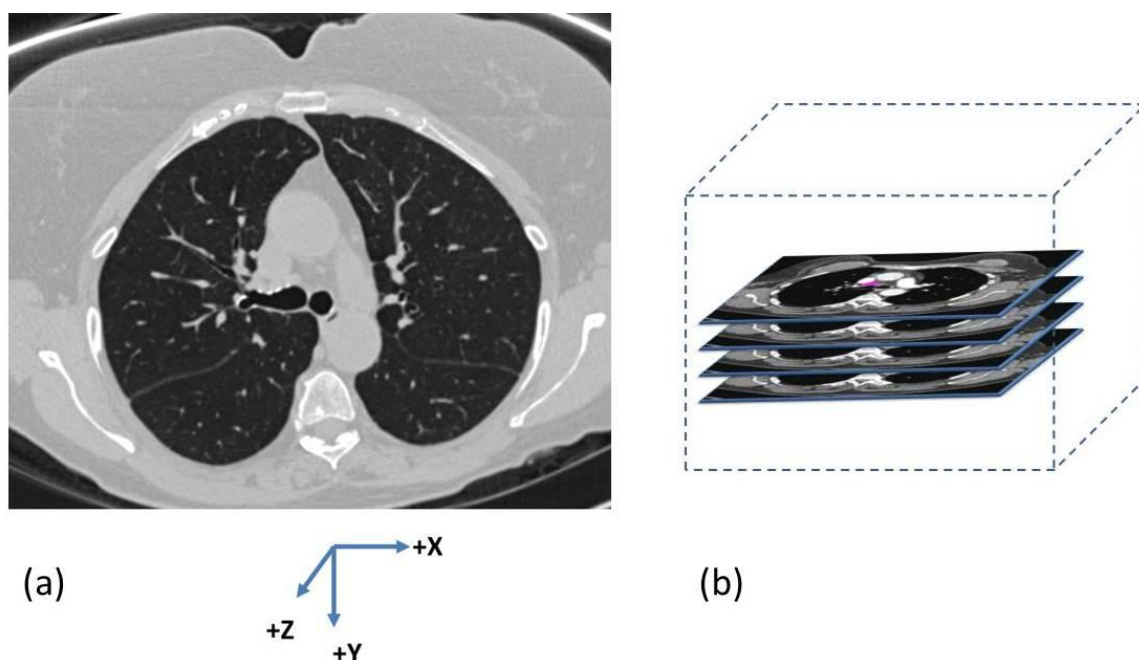


Figure 1.1: Volume representation by individual slices. (a) A single slice. (b) Multiple slices representing the chest volume.

The axes are oriented so that +x points to the patient's left, +y points to the patient's back, and +z points to the patient's feet.

Originally, the analog and digital images were mutually exclusive; that is, analog representations could not be extracted from the digital images. This is not the case at present, as modern computing techniques have brought many options for reconstruction from a digital CT scan [3].

Advancements in CT technology have allowed for sub-millimeter resolution, which allows for the visualization of nearly all airways in the lungs [6, 13, 14]. After building on the technology of the original single-detector CT scanners, multi-detector row computed technology has led to the ability to view images in multiple planes, as opposed to the single axial plane allowed by traditional CT [8]. This imaging technology has led to the ability to generate three-dimensional anatomical renderings using various image processing techniques, depending on the

anatomical structures of interest. As image resolution and rendering techniques continue to improve, possibilities continue to emerge in coupling clinical care and medical image processing.

The Multidimensional Image Processing Lab (MIPL) has developed a software package which is capable of taking a high resolution MDCT chest scan as input and producing a three-dimensional rendering of the airway tree while extracting other pertinent information for the purpose of improving the efficacy of clinical bronchoscopy procedures via real-time navigation [7]. We are specifically interested in the main data file output by the software suite: the .npth file. The .npth file contains all quantitative information needed to perform our analysis.

While the quantitative information is used in various applications within the MIPL software suite, a comprehensive compilation of these quantitative measurements has not been performed using this set of data. A quantitative analysis of this data may help improve current bronchoscopy techniques in route planning and device selection. For this reason, we take interest in extracting the information contained within these specialized quantitative data files, and sorting and grouping them to allow for observation of trends and anomalies within a patient population with respect to the airway tree anatomy.

Chapter 2 provides a background on the anatomy of the human lung, explaining pertinent anatomical considerations such as lobe characterization and the definition of a branch as the fundamental unit of the airway tree. Chapter 3 gives an explanation of the methods used to process the input images and produce the graphs and tables displayed in Chapter 4. In addition to containing the resultant graphs and tables, Chapter 4 provides results and explanations of observations made from the analysis. Chapter 5 then sums up general conclusions and provides brief commentary on potential future endeavors.

Chapter 2

Anatomy of the Human Lung

In order to motivate and orient our study, we first present an anatomical overview of the human lung. The lungs are divided into anatomically separate units called lobes as explained in Section 2.2, though this representation alone is not much use to our study as it explains little of the interior of the lungs. Because this study deals with the airway tree and not with the surrounding tissue, we will focus particular attention on the structures that comprise the gas-exchange structures within the lung. This requires us to look at the branch, the basic anatomical unit of the airway tree, and how it connects with other branches to form a full tree. This representation is explained in Section 2.2. We have also made assignments to allow for consistent labeling across a large number of cases, explained in Section 2.3.

2.1: Top-Level Lung Anatomy

The lung is an organ which functions as the site of gas exchange in many vertebrate organisms [1]. Most importantly, the organ acts to enrich blood with oxygen while allowing carbon dioxide to be removed, a function vital to human life. In normal anatomical instances there are two lungs, one lying on each side of the heart within the thoracic cavity. Because the heart occupies more space to the left of the sternum, the right lung tends to be larger than the left. This is demonstrated by the fact that the right lung consists of three lobes and the left consists of just two. These lobes are physically separated from one another by interlobar fissures. The left lung, while only containing two true lobes, contains a section of interest called the lingula which

may be identified in normal anatomical conditions. This lobar representation of the human lungs is demonstrated in Figure 2.1.

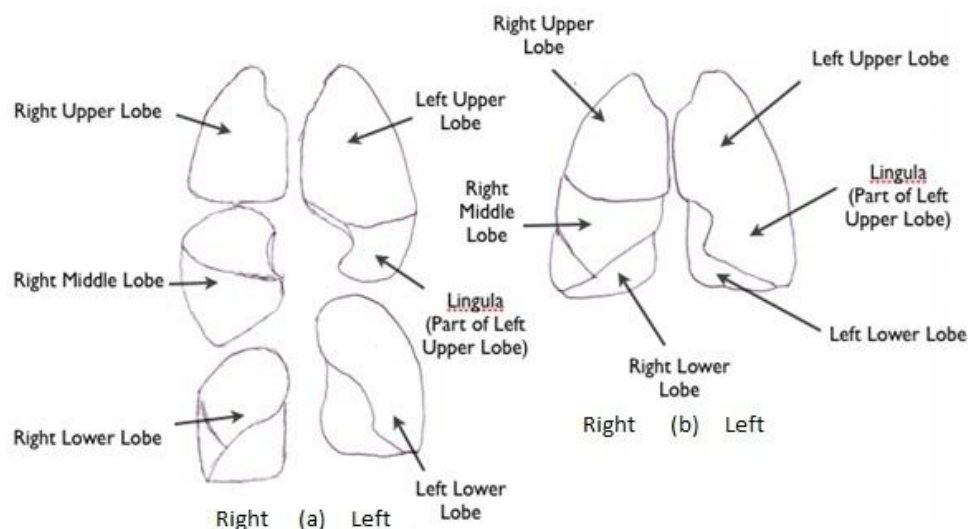


Figure 2.1: Lobes (and lingula) of the human lung. (a) Lobes are separated to show relative size and shape. (b) Lobes are connected as in normal anatomy to show full lung structure.

While our study focuses on the airway tree rather than the exterior surfaces of the lung, the airways described in Section 2.2 may be separated into groups by lobe, allowing for comparison of the branches contained within each lobe (i.e., left lower lobe versus right lower lobe).

2.2: Branch Representation

While the lobar representation provides a nice outer anatomical view of the organ, it does little to help explain the physiology of the air exchange inside of the lung. The lung is essentially an empty sac that is subdivided into lobes and inflates with air upon inhalation [1]. In addition to the air-containing structures, there is an extensive vascular tree which supplies the lung tissue with blood. For our study, only the air-containing structures of the lung are to be considered. The

functional interior of the lung with respect to air exchange is a compartmental structure that may be divided into discrete airway units called branches, which in aggregate connect to form a tree structure, referred to as an airway tree [1]. A single branch is an approximately cylindrical segment defined to extend from its proximal origination at a bifurcation from its parent branch to its distal termination in one of two ways: either a bifurcation into two daughter cells (for a non-terminal branch) or connection to an alveolar sac (for a terminal branch), which is the primary air exchange structure present in the lung. This definition of a branch is illustrated in Figure 2.2.

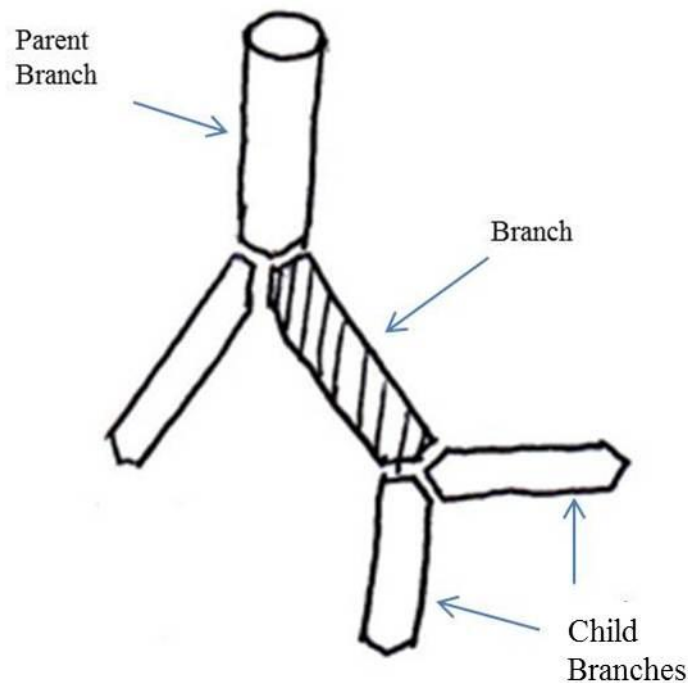


Figure 2.2: Illustration of a single branch (shaded) as it connects to its proximal parent and distal daughter branches.

2.3: Branching Pattern

For our study, we adopt a specific branching pattern which dictates many of the logical decisions made in Chapter 3. When considered together, the branches form a tree structure

beginning with a single trunk called the trachea and terminating in the alveolar sacs [1]. The trachea splits into two main bronchi: the right main bronchus and the left main bronchus. The right and left main bronchi conduct air into the right and left lungs, respectively. Because of the position of the heart, the left main bronchus is normally longer than the right main bronchus.

The left main bronchus then bifurcates into two bronchioles: the left upper lobe parent branch and the left lower lobe parent branch. The right main bronchus also bifurcates into two bronchioles: the right upper lobe parent branch and the right intermediary bronchus. The right intermediary bronchus then branches into the right middle lobe parent and the right lower lobe parent. The right upper lobe parent feeds (conducts air) into the right upper lobe, while the right middle and lower lobe parents feed into the right middle and lower lobes, respectively. The left upper lobe is also the parent of the lingula parent. This branching pattern continues until termination in an alveolar sac. Because each branch splits into two constituent branches, there are approximately 2^n branches in generation n (where generation 0 is the trachea). This standard branching pattern is illustrated in Figure 2.3. Figure 2.4 points out these branches in a 3D rendering.

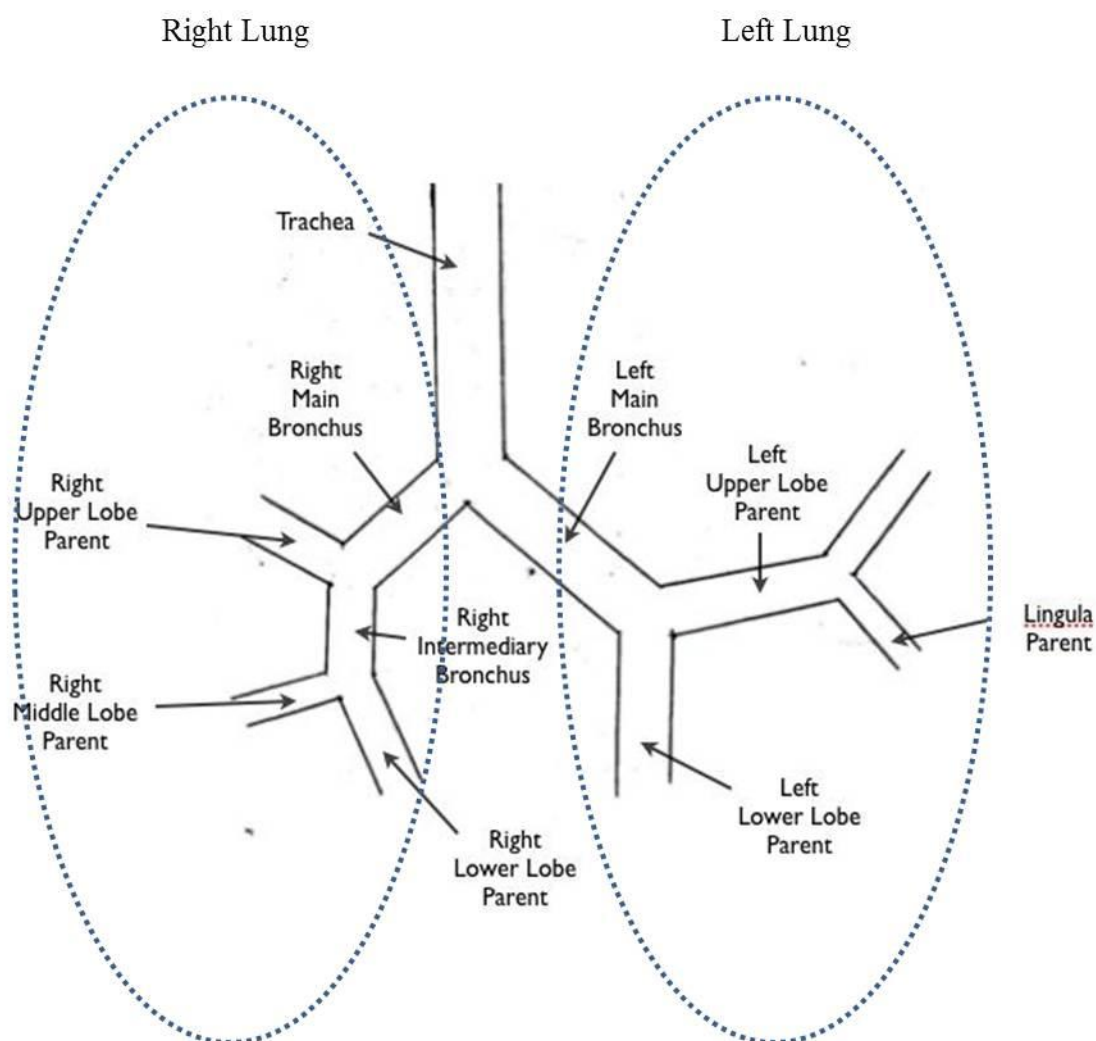


Figure 2.3: Branching pattern of the trachea (generation 0), main bronchi (generation 1), five lobar parents, right intermediary bronchus, and lingula parent. The dotted ovals represent the rough outlines of the right and left lungs.

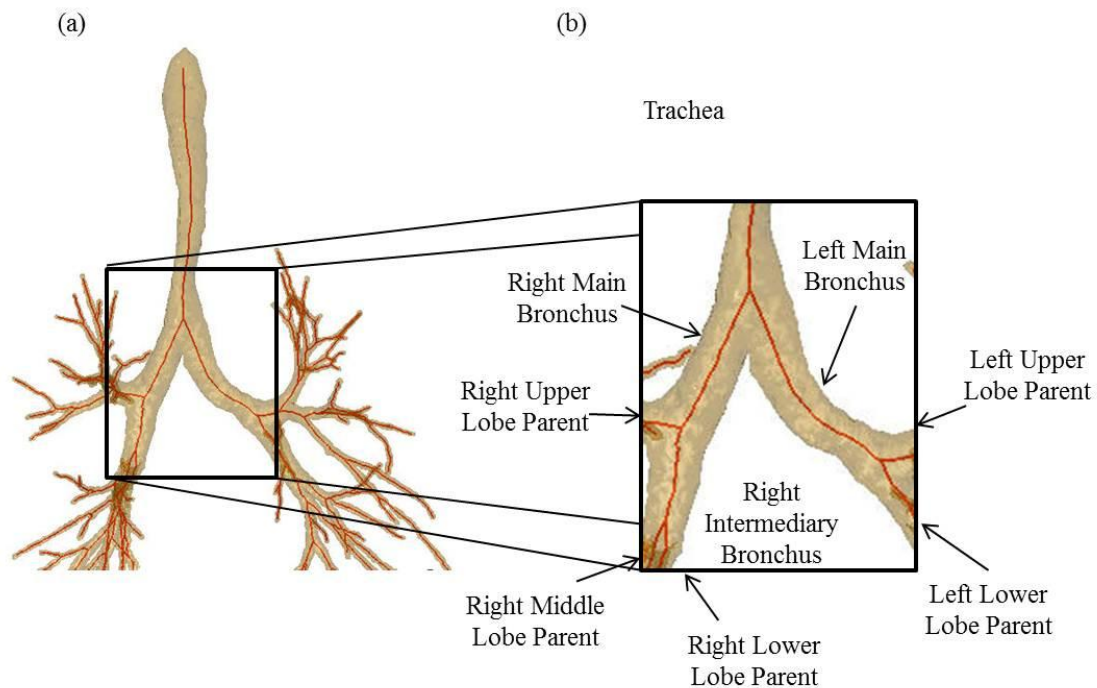


Figure 2.4: Branching pattern illustrated in the 3D rendering of patient 20349_3_55. (a) The entire tree is shown. (b) The airways of the hilum are expanded and key branches identified.

We note that the human airway tree does not exhibit regular dichotomy [1]. In a normal dichotomy, conjugate branches, or branches originating from the same parent, have equal length and diameter dimensions, and leave the parent branch at the same angle. According to Weibel, studies of the airways have shown that conjugate branches often do not have equal dimensions, and that the airway does not follow a regular dichotomy. It has also been shown that the branch angle is proportional to the dimensions of the conjugate branches; small branches tend to originate at an angle more near 90° , while large branches tend to originate at an angle closer to 0° [1].

Ewald Weibel's study found that the average generation at which terminal airways lie is generation 23, where the trachea is generation 0. Weibel indicates that the terminal airways are in fact distributed over a range of subsequent generations, though at the time of his study no method

was available to estimate the distribution. As a size comparison between generations, the trachea is approximately 2 cm in diameter, while an alveolar duct or sac is approximately 200-600 μm in diameter [1].

Chapter 3

Methods

In order to perform the desired quantitative analysis, the pre-existing image data from the MIPL must be in some way sorted and oriented into a usable format. As mentioned in Section 1.2, the current MIPL software suite takes an image as input and produces among other things a three-dimensional surface rendering and .npth file containing the dimensions of all branches identified within the tree. To create a usable format for quantitative analysis, we developed two programs which allowed for the ultimate formulation of graphs and tables.

The first program, called “BranchStats” (Section 3.2), is a variant of the DiameterColorDialog developed by Duane Cornish [7]. BranchStats operates on a single case and must be run on every case included in the study. Using information from the input .npth file, the program makes multiple logical decisions and performs several calculations to formulate a number of quantitative and qualitative metrics for each branch contained within the case. These metrics are then written to an output file, creating a succinct, standardized text file, called the “BranchData” file (Section 3.2). This program completes the analysis for a single case. The BranchData file contains a tabular representation of statistical information about all branches contained within the case study and is used as the input for the second program. The process for single case analysis is shown in Figure 3.1.

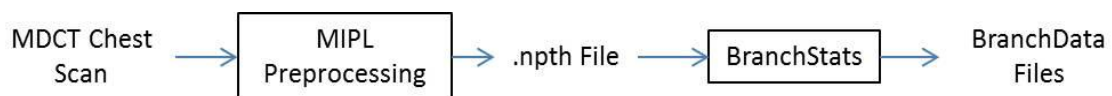


Figure 3.1: Flow chart showing single case analysis. The input is an image file and the output is a BranchData text file. The .npth file is created as an intermediate and serves as the input to BranchStats.

The second program, explained in Section 3.3, is a MATLAB program which may be run on an entire population of cases at once. Each case must have a properly formatted BranchData text file associated with it. The program accepts a directory filled with BranchData text files as input, calculates a number of statistics from the data contained within all of the BranchData files, and writes an aggregate statistical analysis (Analysis) file as output. The Analysis file is then opened in Microsoft Excel, where we create a number of graphs and tables to represent the calculated data from the given population. The process for multi-case analysis is shown in Figure 3.2.



Figure 3.2: Flow chart showing multi-case analysis. The input is a directory folder of BranchData text files and the output is in the form of Excel graphs and tables. The Analysis file is generated as an intermediate.

The qualitative and quantitative fields to be studied are dictated by the .npth file and by anonymized patient information stored over the course of MIPL research. The metrics stored in the .npth file identify individual branches (i.e., branch length, average branch diameter), while others identify all branches within a patient's airway tree, such as patient gender and body mass index (BMI). BMI is defined as weight in kilograms divided by the square of height in meters [9].

These metrics allow for observation of branch dimensions (length, diameter, and angle with parent) both globally (using the entire population) and within sub groups (male versus female, BMI category). This in turn provides a useful presentation for the analysis of consistencies and differences among groupings, in addition to the indiscriminate global anatomical analysis.

3.1: MIPL Preprocessing

This section describes the process of beginning single-case analysis using the MIPL software suite. This standard preprocessing method is used for all cases by the MIPL [7]. MIPL preprocessing takes an input image file and creates several outputs. The .npth file is of particular interest in our study. We utilize the following tools from the MIPL software suite in our analysis to build the case and generate the desired .npth file (in order): Virtual Navigator, Seg Tool, Surface Tool, Centerline Tool, and Path Quant Tool [7].

The first step in our analysis was to apply MIPL preprocessing to all images to be considered, as shown in Figure 3.1. Ideally, two kernels arising from two different image reconstruction algorithms are used as input to the MIPL software suite: the B31, a smooth kernel, and the B50, a sharper kernel. These algorithms create chest volume images containing voxels that are $\Delta x = 0.6$ mm by $\Delta y = 0.6$ mm by $\Delta z = 0.75$ mm, with 0.5 mm slice spacing (space between the center of adjacent slices), resulting in approximately 600 slices. This represents a much higher-resolution reconstruction than those with $\Delta z = 3$ mm slice thickness in reconstructions typically used by radiologists; this higher resolution is important to allow the computer algorithms to properly segment the tree, generate smooth surfaces, and calculate accurate quantities. In many instances, the B50 kernel, the B31 kernel, or both were unavailable due to these reconstructions not being obtained at the time the scan was performed. In these instances, the sharper kernel is used for the segmentation while the smoother kernel is used for surface generation, centerline generation, and path quantitation. For cases in which only one kernel is available, the single kernel is used for all facets of preprocessing. These options slightly reduce the quality of the renderings, but still result in usable data.

Once the images are collected, the sharper kernel may be loaded into a case study (.csy) file for use in Virtual Navigator. Before any 3D reconstructions or quantitative data may be used,

they must first be generated by invoking the tools developed by the MIPL. For each case to be considered in the analysis, the case study file must first be segmented via Seg Tool (preferably using a B51 kernel). Once this airway tree segmentation is complete, the tree skeleton must be manually inspected to ensure that it has segmented properly [7].

We note that the Seg Tool does not identify every airway within the lung volume, and to add every airway manually would be impractical. Many branches have dimensions too small to be identified using the available (or any) resolution. In addition, the Seg Tool uses a more conservative approach to segmentation, meaning even some branches that are identified are not included because they do not meet other segmentation criteria as explained in Section 1.2 [6]. This helps to avoid adding false-positive branches, as a false-positive branch creates a bifurcation in the segmentation where there is not one. Because a central focus of the MIPL is navigational bronchoscopy, false bifurcations are unacceptable as they may confuse a physician performing a live procedure.

After segmenting the airway, the smoother kernel (preferably B31) is loaded into the case study in Virtual Navigator. With this image file, the case study file may be run through the Surface Tool, Centerline Tool, and Path Quant tool in order to generate a 3D rendering and .npth file, as mentioned in Section 1.2. Upon completing this process, the case is fully built, and the .npth file is available as input to the BranchStats tool.

Because of the fact that the MIPL tailors its work to applications in guided bronchoscopy, there is a premium on accurate segmentation rather than a liberal addition of potentially false branches which may confuse the physician. In the past, various segmentation methods have correctly identified between 32% and 40% of generation 3 or higher subsegmental branches, which correspond to branches with lobar generation 4 or higher as defined in Section 3.2. Due to the efforts of Michael Graham and the MIPL, that number is now up to 65%, resulting in better and more reliable segmentations [6]. While this is a marked improvement, we must note that this

method still omits 35% of branches lobar generation 4 (approximately global generations 6 and 7) or higher, including segmented branches that do not meet specified cost-benefit criteria. These tend to be smaller branches, as these branches are more difficult to reliably segment due to resolution constrictions. As a result, the airway tree is inherently skewed toward having a larger average branch size than is actually anatomically accurate.

3.2: Completion of Single-Case Analysis

In this section, the C++ code used to complete single-case analysis is explained. The code accepts the .npth file as input and can be broken into two sections. The first section of code makes several logical decisions to identify the key branches illustrated in Figure 2.3. Once these branches are identified, the second section of code iterates through every branch stored in the .npth file and makes logical decisions and calculations based on the information in the .npth file and the key branches. This process is illustrated in the flow chart in Figure 3.3.

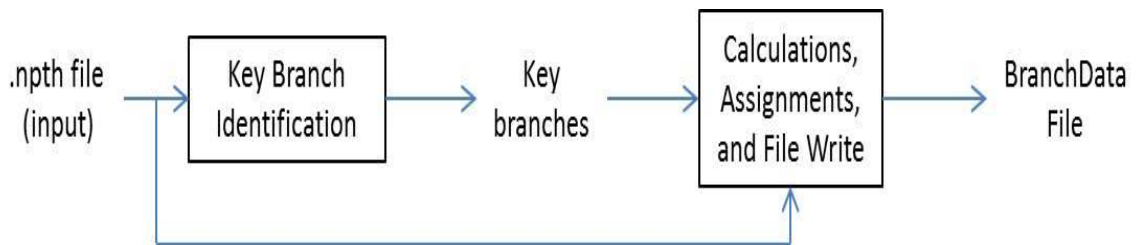


Figure 3.3: Process of creating a BranchData file using an .npth file as input.

Section 3.2.1 explains the process for identifying the key branches. Section 3.2.2 explains the process for calculating and writing the data to the output file.

3.2.1: Key Branch Identification

Each branch in the tree is identified in the .npth file by a branch ID unique to that case, and each branch's parent branch ID is also stored. The file also contains the coordinates of all viewsites along the branch, as well as the inner and outer branch diameters at each viewsite [7]. Branch ID numbering always starts with the trachea, and we observe that every branch's unique integer ID number is greater than that of its parent branch. This is important because if we know the parent branch of branch *n* lies in a particular lung and lobe, we know branch *n* will lie in the same lung and lobe.

We must first identify the lung and lobe parents to be able to identify every branch by lung and lobe (including lingula), and to calculate lobar generation number (explained in Section 3.2.2). Identification can be summed up in the following nine steps:

1. Identify branch IDs of the daughters of the trachea, which are the right and left main bronchus (Figure 2.3).
2. Identify which trachea daughter is the right main bronchus and which is the left
3. Identify branch IDs of the daughters of the two main bronchi. The left bronchus's daughters are the left upper lobe parent and the left lower lobe parent, while the right bronchus's daughters are the right intermediary bronchus and right upper lobe parent (Figure 2.3).
4. Identify which right main bronchus daughter is the right upper lobe parent and which is the right intermediary bronchus.
5. Identify which left main bronchus daughter is the left upper lobe parent and which is the left lower lobe parent.

6. Identify branch IDs of the daughters of the right intermediary bronchus. The daughters of the right intermediary bronchus are the right middle lobe parent and right lower lobe parent (Figure 2.3).
7. Decide which right intermediary bronchus daughter is the right lower lobe parent and which is the right middle lobe parent.
8. Identify branch IDs of the daughters of the left upper lobe parent. One daughter of the left upper lobe parent is the lingula (Figure 2.3).
9. Identify lingula parent.

Each step in the list represents a section of C++ code. All steps can be accomplished using the information stored in the .nph file. Full identification of the key branches required the use of three arrays corresponding to three qualitative identifiers for each branch: lung, lobe, and label. The lung identifier for a particular branch is designated “L” or “R” if the branch is in the left lung or right lung, respectively. The lobe identifier for a branch is assigned “U,” “M,” or “L,” for upper, middle, or lower lobe. This combined with the lung value tells us which lobe contains the branch. The label identifier is reserved for the key branches identified in Figure 2.3 and lingula branches. The trachea is assigned both lung and lobe values of “N/A,” as it lies between the lungs. The trachea is also assigned the label “T.” The logical decision points for each of the nine steps are as follows:

1. This section of code checks the parent branch ID of every branch. If the parent branch ID is 0 (trachea), the branch is a main bronchus and is assigned the label “MB.”

2. Because the left main bronchus is longer than the right, we simply compared the number of viewsites in the two main bronchi. The main bronchus with fewer viewsites is shorter and is designated the right main bronchus by assigning a lung value of “R.” The other main bronchus is designated the left main bronchus by assigning “L” as its lung value.
3. Like the first step, this section checks the parent branch ID of every branch in the case. If the parent branch ID matches either of the main bronchus branch IDs, the code then checks the lung value of the parent branch. The two right main bronchus daughter IDs are stored for step 4, and the two left main bronchus daughter IDs are stored for step 5.
4. This section of code makes the assumption that the right upper lobe parent is superior to the right intermediary bronchus, as in Figure 2.3. To check superiority, the z value of the third viewsite of each branch is compared. The branch with the more positive third-viewsite z value is more inferior (Figure 1.1) and is designated the right intermediary bronchus. This branch is assigned a lung value of “R,” a lobe value of “N/A,” and a label of “IB” (for intermediary bronchus). The branch with the more negative z value is more superior and is designated the right upper lobe parent. This branch is assigned a lung value of “R,” a lobe value of “U,” and a label of “UP,” for upper parent.

5. In this step, we assume the left upper lobe parent is superior to the left lower lobe parent. As in step 4, superiority is checked using the third viewsite of each branch. The left main bronchus daughter with the more positive third viewsite z value is designated the left lower lobe with a lung value of “L,” a lobe value of “L,” and a label of “LP” for lower parent. The other left main bronchus daughter is designated the left upper lobe with a lung value of “L,” a lobe value of “U,” and a label of “UP” for upper parent.
6. As in steps 1 and 3, step 6 checks the parent branch ID of every branch present. The two daughters of the right intermediary bronchus are stored for step 7.
7. This section of code compares the z value of the third viewsite of each of the right intermediary bronchus daughters, much like in steps 4 and 5. The more superior branch is designated the right middle lobe parent with a lung value of “R,” a lobe value of “M,” and a label of “MP” for middle parent. The more inferior branch is designated the right lower lobe parent with a lung value of “R,” a lobe value of “L,” and a label of “LP” for lower parent.
8. Like steps 1, 3 and 6, this section of code checks the parent branch of all branches. The two daughters of the left upper lobe parent are stored for step 9.
9. As in steps 4, 5 and 7, this section of code compares the z value of the third viewsite of the two branches in question. The more inferior branch is designated the lingula parent with a lung value of “L,” a lobe value of “U” (Figure 2.3), and a label of “LingPar” for lingula parent.

Once these branches have been identified, we have all information necessary to label all branches and calculate the desired statistics, as explained in Section 3.2.2.

3.2.2: Writing the Output File

This section explains the procedure for calculating all statistics and assigning all labels to be written to the output file, called the BranchData file. In the BranchData file, every branch contains a value for every metric. This allows us to perform the same calculations on every branch, so we use a loop to iterate through all of the branches. Within the loop, we assign each metric to a corresponding array indexed by the branch ID, which is also the current iteration of the loop. This allows for consistent indexing for both assignment and writing. Once the metrics are assigned for a single branch within a single iteration of the loop, the program writes them to the BranchData file in a single row separated by tabs. The 10 metrics to be assigned and written to the output file are as follows:

1. Branch ID: Each branch is assigned a unique ID within the .npth file. Branches are simply numbered beginning with the trachea at branch ID zero. As mentioned in Section 3.2.1, no branch has an ID number lower than its parent. This is of particular importance because it ensures that all values for the parent branch are calculated and may be called by the daughter. For example, branch n will always have the same lung laterality as its parent branch, a value which will be known at the time that branch n is in the loop due to its higher ID.
2. Number of Viewsites: This number is stored in the .npth file for each branch.

3. **Generation Number:** Like branch ID, this number is explicitly stored within the .npth file. Because each branch's parents are known, the generation number of branch n is equal to the generation number of its parent branch plus one.
4. **Lobar Generation Number:** This number is calculated within the loop, as it is an assignment devised specifically for this study. The five lobar parents are each assigned lobar generation number one, the daughters of these five are designated lobar generation two, and so on. The trachea, main bronchi, and right intermediary bronchus are assigned a value of zero for lobar generation, an arbitrary designation as no true lobar generation as defined here exists. This numbering convention allows for a more like-to-like comparison, as right lower and middle lobe branches are inherently skewed toward a higher raw generation number. This is due to the fact that these lobes lie distal to the right intermediary bronchus, thus adding an inherent generation to all constituent lobar branches.
5. **Average Diameter:** The .npth file specifies a maximum and minimum inner diameter for each viewsite within a given branch. The mean of these two numbers is calculated for every viewsite and summed with all other viewsite means from the branch. The sum is then divided by the number of viewsites to give an average branch diameter.
6. **Branch Length:** The distance between each pair of adjacent viewsites is calculated from the position information in the .npth file and summed to give total branch length.

7. **Angle with Parent:** Two angle with parent calculations are performed. In the first, a vector is created from the first to the third viewsite of the current branch. If the branch is two viewsites long, the vector is created from the first to the second viewsite. If the branch is one viewsite long, no angle will be calculated as a vector cannot be created in this branch, and it is arbitrarily assigned a branch angle of “-1.” Next, a vector is created from the third-most-distal viewsite in the parent branch to the most distal viewsite in the parent branch. If the parent branch is two viewsites long, the vector is created from the second-most-distal to the most distal viewsites, and if the parent branch is only one viewsite long, again no angle will be calculated as a vector cannot be created within the branch. If two vectors are obtained, the angle is calculated from the dot product of the two vectors. The second angle with parent calculation is the same as the first, except it uses the first and fifth viewsites of the daughter branch and the fifth-most-distal and most distal viewsites of the parent branch. If a branch is fewer than five viewsites but more than one, the longest vector possible is made pointing in the distal direction. We note that these vectors are always created with the head at the distal end so that a branch continuing in the same direction as its parent has an angle with parent of 0.

8. **Lung Laterality:** With the exception of the two main bronchi, each branch is assigned the same lung value as its parent branch. As mentioned before, a parent branch must always have a lower branch ID than its daughters, ensuring the parent is assigned a lung value first. The trachea is assigned a lung value of “N/A.”

9. **Lobe Characterization:** Each branch distal to the lobar parents is assigned the same lobe value as its parent branch. Again, a lower parent branch ID ensures a value will be

present. The trachea, main bronchi, and right intermediary bronchus are assigned a lobe value of “N/A.”

10. Label: Before the output file loop, the trachea, main bronchi, lobar parents, and lingula parent are all assigned a special label value. With the exception of lingula branches, all other branches are assigned a value of “N/A.” All branches with a parent label of “LingPar” (for the lingula parent) or “Ling” are assigned a label of “Ling” to designate that they are lingular branches.

After assigning all of the metrics for a given branch within the loop, an output command line writes all of the metrics to a single row in the output file. Once the loop has finished iterating through all branches present in the current case study file, the program closes the output BranchData file and terminates.

3.3: Multi-Case Analysis

This section details the process of taking a group of BranchData files and creating the output graphs and tables. This requires two main steps: processing the BranchData files in MATLAB to create an intermediate Analysis file and processing the Analysis file in Microsoft Excel to produce the desired figures and tables. A top-level view of the process is shown in Figure 3.4.

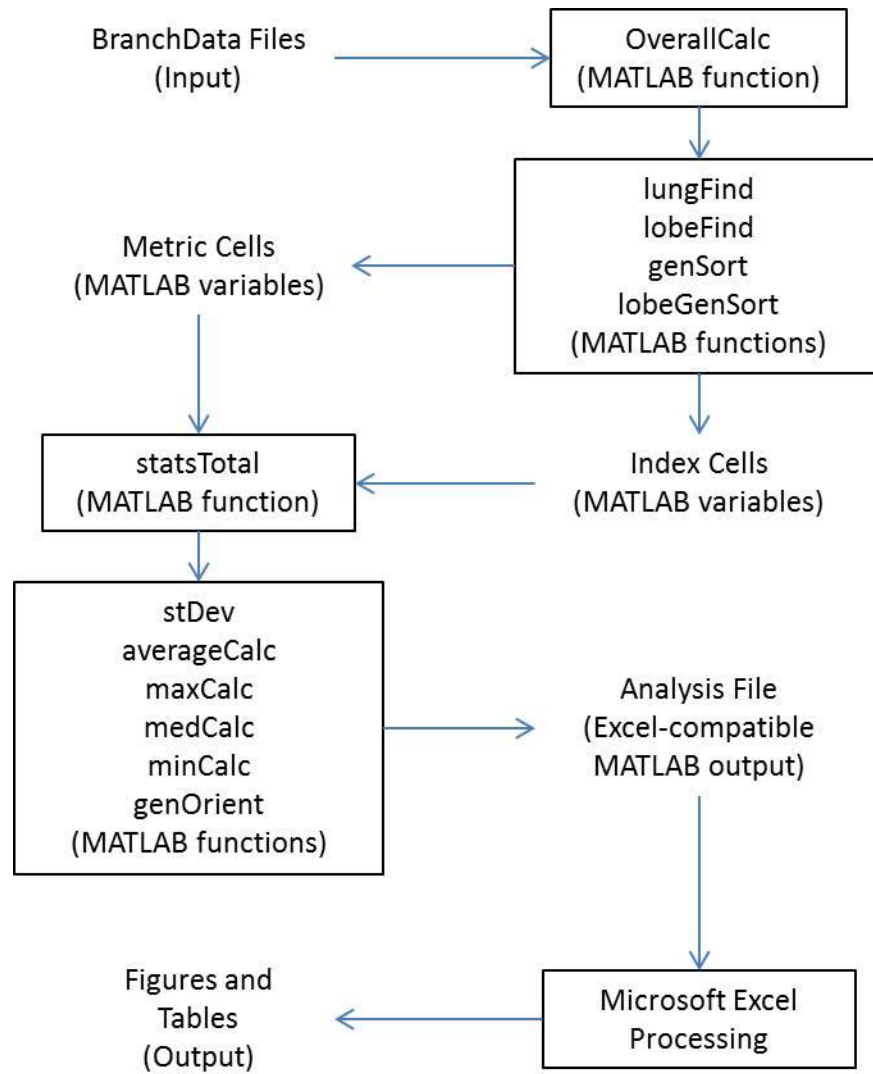


Figure 3.4: Multi-case analysis process.

Section 3.3.1 details the MATLAB program written to create the intermediate, Microsoft Excel-compatible Analysis file. Section 3.3.2 explains the graphs and tables we create from the Analysis file.

3.3.1: Creating the Analysis File

After creating BranchData text files for all of the individual cases, we created a program to read, group, and compute statistics on the data within the text files, then write them to an output “Analysis” file. There are twelve functions necessary for our MATLAB program to run properly. The main function, “OverallCalc,” iterates through each BranchData file contained in the input directory and calls four functions to create “index arrays,” which are then stored in “index cells.” These index cells are sent with “metric arrays” stored in “metric cells” to statsTotal. StatsTotal then uses these arrays to write a coherent output Analysis file.

The input directory dictates the population contained in the Analysis file. We create seven Analysis files in our study: One for the entire population, one for each gender, and one for each of the four BMI classifications [9].

In order to use the data in the BranchData files, the data must first be stored in a MATLAB variable. To do this, we read one BranchData text file into a single cell structure. Each column of the cell represents a different metric in the BranchData file (Section 3.2) and each row represents a single branch. This cell is then split into eleven nx1 cells. Each nx1 cell contains a single column of the original cell (where n equals the total number of branches in the tree). The most useful caveat to using this method is that each nx1 cell’s values stay indexed exactly how the branch ID cell is indexed. For example, to call the branch diameter of branch 254, one need simply call item 254 from the branch diameter cell.

After storing the data in cell structures, OverallCalc calls four functions to sort the branches in the case into different categories. These four functions are named “lungFind,” “lobeFind,” “genSort,” and “lobeGenSort.” Each function receives one or more input cell and creates one or more index arrays. The four functions are explained briefly as follows:

1. lungFind: This function accepts the Lung cell as input and creates two output arrays: “leftbranches” and “rightbranches.” Leftbranches contains a list of all left lung branch IDs, while rightbranches contains a list of all right lung branch IDs.
2. lobeFind: This function accepts the Lobe, Lung, and Label cells as input and creates six arrays as output: “LUbranches,” “LLbranches,” “RUbranches,” “RMbranches,” “RLbranches,” and “LingBranches.” LUbranches contains a list of all left upper lobe branch IDs, LLbranches contains all left lower lobe branch IDs, RUbranches contains all right upper lobe branch IDs, RMbranches contains all right middle lobe branch IDs, RLbranches contains all right lower lobe branch IDs, and LingBranches contains the branch IDs of all lingula branches.
3. genSort: This function accepts the Generation Number, Lung and Label cells as input and creates three outputs: branchGenArray, LMBtemp and RMBtemp.
BranchGenArray is an $m \times n$ array where m is the highest generation present in the case and n is the highest number of branches in any one generation. Each row of the array contains the branch IDs of all branches in that particular generation. For example, row 6 will contain all generation 6 branches’ branch IDs. LMBtemp and RMBtemp are the branch IDs of the left main bronchus and right main bronchus, respectively.
4. lobeGenSort: This function takes the Lobar Generation Number cell as input and creates a lobeGenArray as output. The lobeGenArray produced is the same as the branchGenArray, except each row now represents a lobar generation number rather than a raw generation number.

Once these 10 index arrays have been created for the case, they are stored in 10 different index cells. The array’s position within the cell is the same for all 10 arrays, and identifies the

array based on the current BranchData file. The first BranchData file in the input directory occupies position one for all index cells, the second occupied position two, and so on. The branch IDs contained within the index arrays serve as pointers to select the correct values from the following arrays: generation number, average diameter, branch length, and both 3- and 5-point angle with parent branch, all of which are “metric arrays.”

Metric arrays contain values for every branch in the current case. This allows for coupling with an index array to perform an operation on only a subgroup of the entire case. For example, if we take the mean of the average diameter array, which contains the average diameter of every branch in the case, we get the mean average diameter for the entire case. If we take the mean of only the values at indices indicated by leftbranches, however, we get the mean average diameter for just branches in the left lung. The metric arrays are stored in metric cells in the same fashion as index arrays are stored in index cells.

This operation is repeated for every case in the input directory. Once this is done, the metric and index cells are sent to statsTotal, where statistics are calculated and written to the output file. StatsTotal calls the remaining six functions to calculate the desired statistics, then writes them to the Analysis file. The eight statistics we display in the Analysis file are the mean, median, maximum, minimum, standard deviation, variance, 5th percentile, and 95th percentile. All values except for variance are calculated by the functions averageCalc (mean, 5th and 95th percentiles), medCalc (median), maxCalc (maximum), minCalc (minimum), and stDev (standard deviation). Variance is simply calculated as the square of the standard deviation. These statistics are calculated for the generation number, average diameter, branch length, 3-point angle with parent, and 5-point angle with parent (meaning each of these five metrics will have each of the eight statistics associated with it). This is done first for the entire tree, then for each of the five lobes and lingula, each generation number, each lobar generation number, and for the left main bronchus and right main bronchus.

The five statistic-calculating functions called by statsTotal all have the same input and output format, as well as the same general operations. Each receives both an index cell and a metric cell as input. Each function then uses two loops to create an array of all desired branches. The outer loop iterates through all cases present, and the current iteration is used to specify which arrays to use from the index and metric cells. The inner loop creates a “calculation array” containing the metric array values at all positions specified in the index array for the current inner-loop iteration. This is done for all cases using the same calculation array. We then perform the desired calculation on the calculation array. While MATLAB contains functions which perform the desired operations, we provide equations for calculating the mean and standard deviation of a set of n values. The equation for calculating the mean, \bar{x} , of n values is given in Equation 3.1.

$$\bar{x} = \frac{\sum_{i=1}^n x_i}{n}$$

Equation 3.1: Equation for calculating the mean of a set of n values.

The equation for calculating the standard deviation, σ , of a set of n numbers is given in Equation 3.2.

$$\sigma = \sqrt{\frac{\sum_{i=1}^n (x_i - \bar{x})^2}{n}}$$

Equation 3.2: Equation for calculating the standard deviation of a set of n values.

For the statistic-calculating functions to run properly, the inputs must be cells containing single-column arrays. Because both the branch generation and lobar generation cells consist of $m \times n$ arrays, they must be reformatted to allow for calculation of statistics. The function “genOrient” was created for this reason. GenOrient creates a single index cell composed of n cells, where n is the maximum generation in the population. Each of these constituent cells, or “generation cells” is composed of m “case cells”, where m is the number of cases which contain branches in that generation. Each of these case cells is composed of the branch IDs of all branches in the generation corresponding to the generation cell. As such, the generation cells may serve as input to the statistic-calculating functions. All statistics are written to the output file (along with the number of branches contained within the subgrouping of branches). A snapshot of an analysis file is shown in Figure 3.5.

	A	B	C	D	E	F	G	H	I
1	Entire Tree	Num of Branches:	20380						
2		Mean	Median	Max	Min	Std Dev	Variance	5th Percentile	95th Percentile
3	Generation	8	8	23	1	2.31	5.36	4	12
4	Avg Diameter	4.41	3.68	23.36	2.27	2.28	5.18	2.75	9.06
5	Branch Length	14.75	12	131.04	0.03	11.53	133	3.21	34.71
6	3-Point Angle with Parent	39.07	36.35	178.27	0.08	21.22	450.2	10.27	75.19
7	5-Point Angle with Parent	38.49	35.71	178.79	0.05	20.31	412.48	11.47	73.28
8									
9	Lingular	Num of Branches:	1254						
10		Mean	Median	Max	Min	Std Dev	Variance	5th Percentile	95th Percentile
11	Generation	6.85	7	11	4	1.48	2.19	4	9
12	Avg Diameter	4.13	3.69	13.66	2.35	1.52	2.31	2.77	7.39
13	Branch Length	15.63	12.44	102.14	0.11	12.48	155.74	3.33	37.97
14	3-Point Angle with Parent	39.97	36.6	175.58	0.16	21.79	474.7	12.68	78.06
15	5-Point Angle with Parent	39.21	35.98	177.75	0.49	20.56	422.65	13.3	76.06
16									
17	Left Upper Lobe	Num of Branches:	4252						
18		Mean	Median	Max	Min	Std Dev	Variance	5th Percentile	95th Percentile
19	Generation	7.66	8	23	3	2.06	4.25	4	11
20	Avg Diameter	4.23	3.66	16.6	2.35	1.82	3.31	2.74	8.4
21	Branch Length	14.03	11.64	102.14	0.11	10.17	103.33	3.03	32.72
22	3-Point Angle with Parent	38.99	36.24	177.99	0.16	21.54	464.15	10.47	75.85
23	5-Point Angle with Parent	38.45	35.98	177.75	0.05	20.38	415.45	11.42	73.97
24									
25	Left Lower Lobe	Num of Branches:	4537						
26		Mean	Median	Max	Min	Std Dev	Variance	5th Percentile	95th Percentile
27	Generation	7.98	8	16	3	2.14	4.56	4	12
28	Avg Diameter	4.4	3.77	17	2.4	1.83	3.34	2.83	8.55
29	Branch Length	14.81	12.42	98.16	0.11	10.11	102.25	3.33	34.49
30	3-Point Angle with Parent	39.65	36.84	178.27	0.42	21.13	446.33	10.66	76.91
31	5-Point Angle with Parent	38.95	36.11	176.87	0.14	20.2	408.18	11.84	74.62
32									
33	Left Lung	Num of Branches:	8870						
34		Mean	Median	Max	Min	Std Dev	Variance	5th Percentile	95th Percentile
35	Generation	7.77	8	23	2	2.17	4.7	4	11
36	Avg Diameter	4.41	3.73	19.52	2.35	2.05	4.21	2.78	9.05
37	Branch Length	14.81	12.13	102.14	0.11	10.84	117.56	3.19	35.85
38	3-Point Angle with Parent	39.41	36.55	178.27	0.16	21.31	454.19	10.6	76.3
39	5-Point Angle with Parent	38.79	36.11	177.75	0.05	20.28	411.21	11.77	74.4
40									
41	Right Upper Lobe	Num of Branches:	4185						
42		Mean	Median	Max	Min	Std Dev	Variance	5th Percentile	95th Percentile
43	Generation	7.35	7	13	3	1.67	2.78	4	10
44	Avg Diameter	4.2	3.57	21.65	2.31	2.12	4.48	2.7	7.92
45	Branch Length	12.64	10.94	67.48	0.03	7.98	63.69	3.09	27.87
46	3-Point Angle with Parent	39.28	36.78	177.43	0.08	20.8	432.64	10.31	73.23
47	5-Point Angle with Parent	38.89	36.21	178.79	0.13	20.12	404.62	12.33	71.73

Figure 3.5: Snapshot of a single Analysis file. Branches are grouped by the entire tree, by lobe, by generation, by lobar generation. Left main bronchus and right main bronchus statistics are also displayed in the file.

3.3.2: Generating Plots and Tables

After creating the Analysis file, we then generate multiple plots and tables to display the data in a more meaningful format. We created a total of seven Analysis files: one containing all cases used in our study, one for each gender, and one for each of the four BMI categories according to the World Health Organization [9]. In our study, we examine branch diameters, lengths, and angles for each lobe and generation. We do this for all cases in the study, as well as for each analysis file to observe similarities and differences among different patient subgroups. The figures and tables we chose to create are displayed and assessed in Section 4.2.

Chapter 4

Data and Results

Section 4.1 gives a brief overview of the database compiled for our study, supplemented by Appendix A. Section 4.2 gives all plots and tables generated by our analysis, as well as an assessment of the results.

4.1: Database

In total, we observe 81 cases in this study. These cases, identified only by study protocol number, are listed in Appendix A along with several pertinent facts about the case and an image of the 3D airway tree rendering. As mentioned in Section 3.1, each case has at least one chest CT scan from which all processing arises. These data come from multiple navigational bronchoscopy studies performed by the MIPL. An example CT image is shown in Figure 1.1. A sample 3D rendering is shown in Figure 4.1. A snapshot of the branch data contained within the .npth file (Section 3.2) is shown in Figure 4.2.

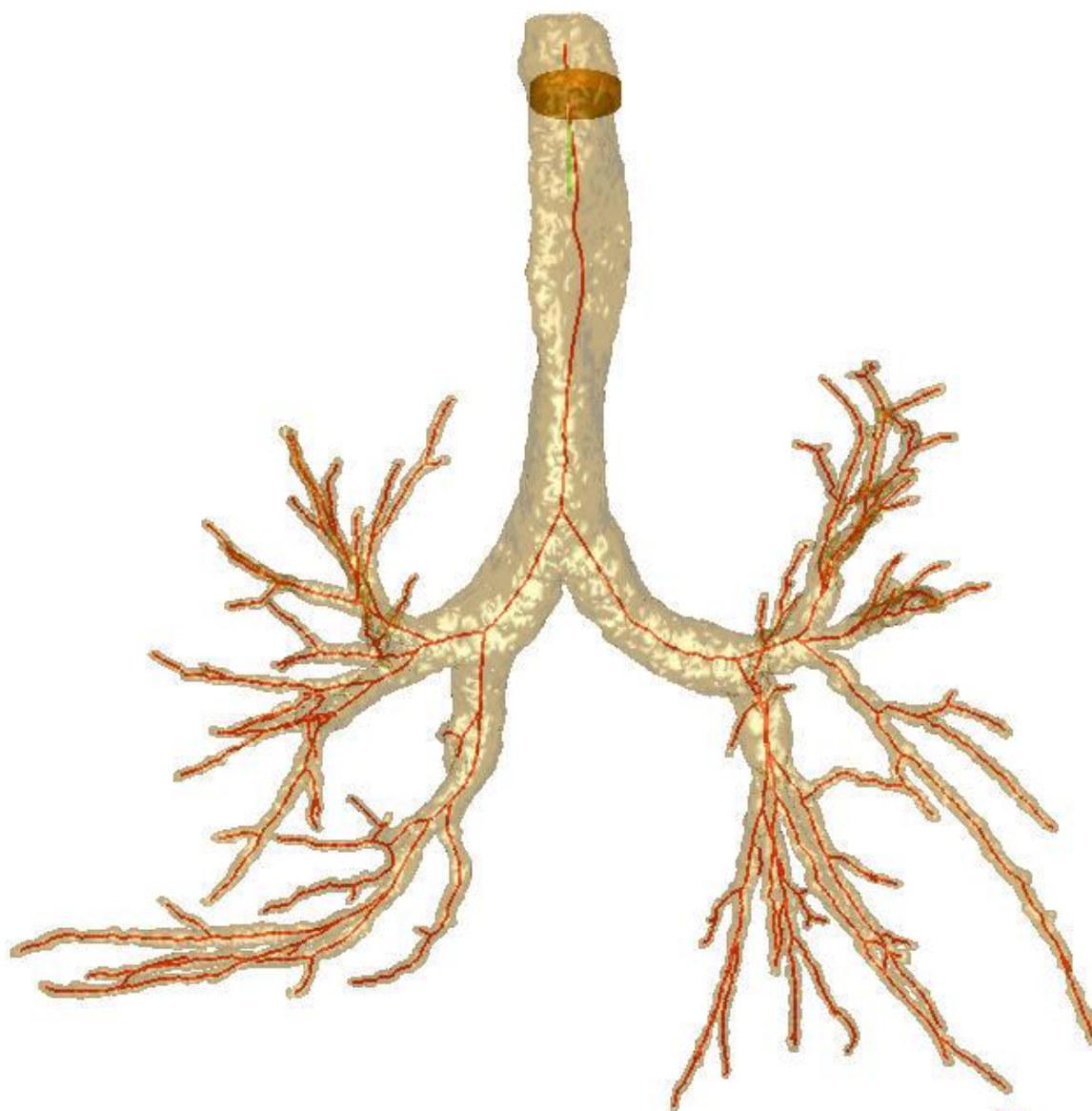


Figure 4.1: 3D rendering of airway tree for case 20349_3_62. The tree contains 223 branches. Processing completed using B31 and B50 images.

```

20349_3_62_B31f - Notepad
File Edit Format View Help

Total_number_of_branches: 223

LIST_OF_VIEWING_SITES_IN_EACH_BRANCH
*****

DATA_FORMAT_FOR_A_VIEWING_SITE
-----

XPOS      YPOS      ZPOS      XANGLE  YANGLE  ZANGLE
BAP      AREA      VOLUME  LABEL   PT_TYPE DTW
MAXODIA  MINODIA  ANGWTR  MAXIDIA MINIDIA MINIDOR

Branch_0
Number_of_viewing_sites 265
Iso_length_of_branch 0.00
Angle_with_parent_branch 0.00
Parent_ID -1

List_of_viewing_sites_in_Branch_0
*****

264.46  213.66   6.78  -21.50  -0.10  -0.00
0.00    203.02   0.00    0        0        0.00
0.00    0.00    0.00   17.22   15.01   0.00

264.43  213.79   7.61  -21.54  -0.09  -0.00
0.00    203.02   0.00    0        0        0.00
0.00    0.00    0.00   17.22   15.01   0.00

264.42  214.02   8.34  -21.53  -0.08  -0.01
0.00    203.02   0.00    0        0        0.00
0.00    0.00    0.00   17.22   15.01   0.00

264.43  214.31   8.99  -21.49  -0.09  -0.00
0.00    203.02   0.00    0        0        0.00
0.00    0.00    0.00   17.22   15.01   0.00

264.45  214.64   9.59  -21.42  -0.10  -0.00
0.00    203.02   0.00    0        0        0.00
0.00    0.00    0.00   17.22   15.01   0.00

264.48  215.00  10.17  -21.35  -0.11   0.00
0.00    203.02   0.00    0        0        0.00
0.00    0.00    0.00   17.22   15.01   0.00

264.53  215.34  10.75  -21.28  -0.13   0.01
0.00    203.02   0.00    0        0        0.00
0.00    0.00    0.00   17.22   15.01   0.00

264.58  215.65  11.35  -21.22  -0.15   0.02
0.00    203.02   0.00    0        0        0.00
0.00    0.00    0.00   17.22   15.01   0.00

264.65  215.91  12.00  -21.19  -0.17   0.03
0.00    203.02   0.00    0        0        0.00
0.00    0.00    0.00   17.22   15.01   0.00

```

Figure 4.2: Sample data in .npth file. The file displays total number of branches in the case, as well as parent branch ID for each branch and the position of all viewsites in the branch. These are the data of importance in Section 3.2. This .npth file corresponds to the tree in Figure 4.1 (20349_3_62).

Two cases, 20349_3_12 and 20349_3_15 (identified in Appendix A by note 3), exhibited an abnormal branching pattern for the daughter branches of the right intermediary bronchus. This is illustrated in Figure 4.3. Figure 4.4 gives an example of a case in Figure 4.3, pointing out relevant branches on the 3D rendering.

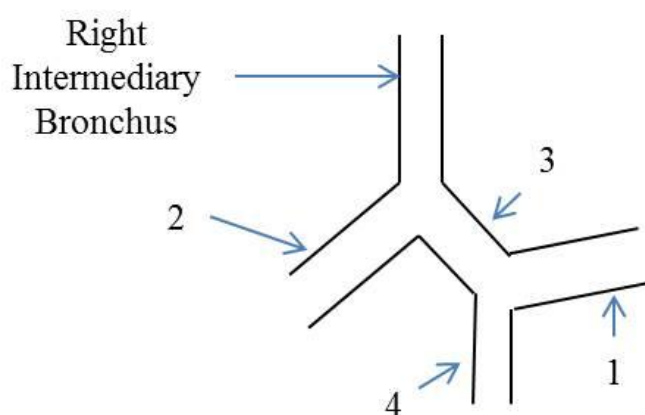


Figure 4.3: Abnormal right middle and lower lobe branching pattern observed in several cases. Branch 1 is the right middle lobe parent, by inspection of interlobar fissures. Branches 2 and 4, however, are both within the right lower lobe. In the BranchData file, branch 2 is designated the right lower lobe parent and branch 1 is designated the right middle lobe parent. Branches 2, 3, 4, and all daughters of branches 2 and 4 are labeled right lower lobe branches, while all daughters of branch 1 are labeled right middle lobe branches.

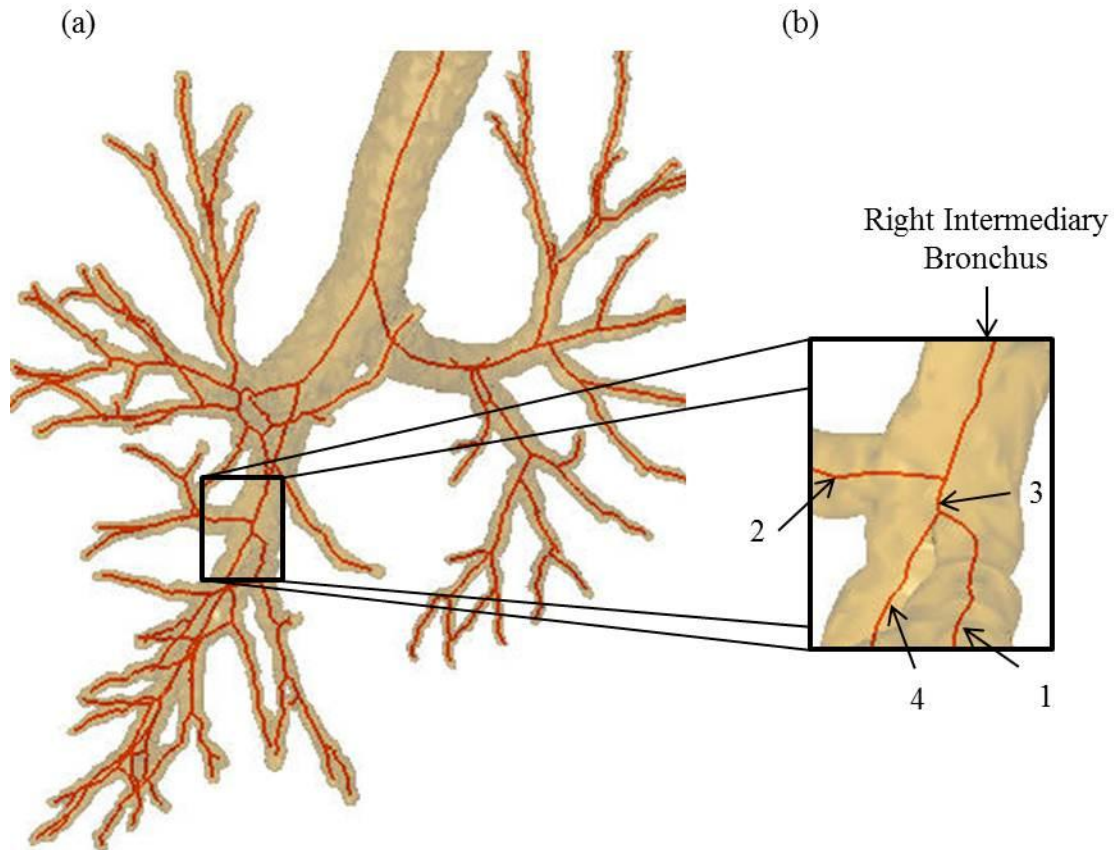


Figure 4.4: Abnormal geometry explained in Figure 4.3. (a) The entire airway tree, rotated to show the right lower and middle lobes. (b) Expanded view of right intermediary bronchus and children in abnormal pattern. The branch numbers used in Figure 4.4 correspond to those used in Figure 4.3.

This allowed us to proceed with generation of results, presented in Section 4.2.

4.2: Results

To help potentially improve route planning and device selection for navigational bronchoscopy, we have created charts and tables of data obtained in our analysis. When navigating to the periphery of the lungs, physicians must select a device which will fit through all airways along the route. Even with an appropriately sized device, a path may contain branches which form angles that may cause difficulty with navigation.

We look at branches grouped by generation, by lobar generation, and by lobe. Based on the assignment of generation numbers, navigating through a path in the airway tree requires the physician to move the scope through each generation in series to arrive at the desired branch. For example, to reach a generation 9 branch, the bronchoscopist must navigate through nine branches (generations 0 through 8) before arriving at the generation 9 branch. Observing branches by generation allows a practical view of the airway tree for a bronchoscopist, as it gives trends related to this approach.

Lobar generation number is nearly linearly related to generation number, but the presence of the right intermediary bronchus (illustrated in Figure 2.3) causes the right lower and middle lobe parents to have a generation number one higher than that of the left upper, left lower, and right upper lobe parents. Viewing data by this grouping allows us to observe how branch characteristics vary as the branches move toward the periphery of the lobes as individual anatomical units.

While observing data by lobar generation gives us a view of trends as branches move into the periphery of the lobes, data is indiscriminate as to which lobe is being represented. We display branch sizes by lobe (and the lingula) in an attempt to observe similarities and differences among the lobes.

We also provide comparisons both by gender and by BMI classification. Observing trends among these groupings may help with procedural planning based on patient demographic, allowing for greater specificity in the planning stages.

Section 4.2.1 details the results obtained from the global analysis (all files included in the study). We observe average branch diameter by generation and lobar generation, branch length by generation and lobar generation, and angle with parent branch by generation and lobar generation. Section 4.2.2 contains a comparison of cases by gender and Section 4.2.3 contains a comparison of cases by BMI.

4.2.1: Global Analysis

Section 4.2.1 focuses on the human airway tree as a whole, rather than observing subpopulations. Grouping all cases into a single analysis allows us to view trends present in the entire airway tree, such as variations in branch dimensions versus generation number or lobar generation number. We first look at average branch diameter, followed by branch length and angle with parent branch. We also compare average diameters and branch lengths to numbers calculated by Ewald Weibel for an airway tree exhibiting a normal dichotomy [1]. Average diameter by generation is illustrated in Figure 4.5 and Table 4.1. A graphical comparison between our calculated means and Weibel's is shown in Figure 4.6.

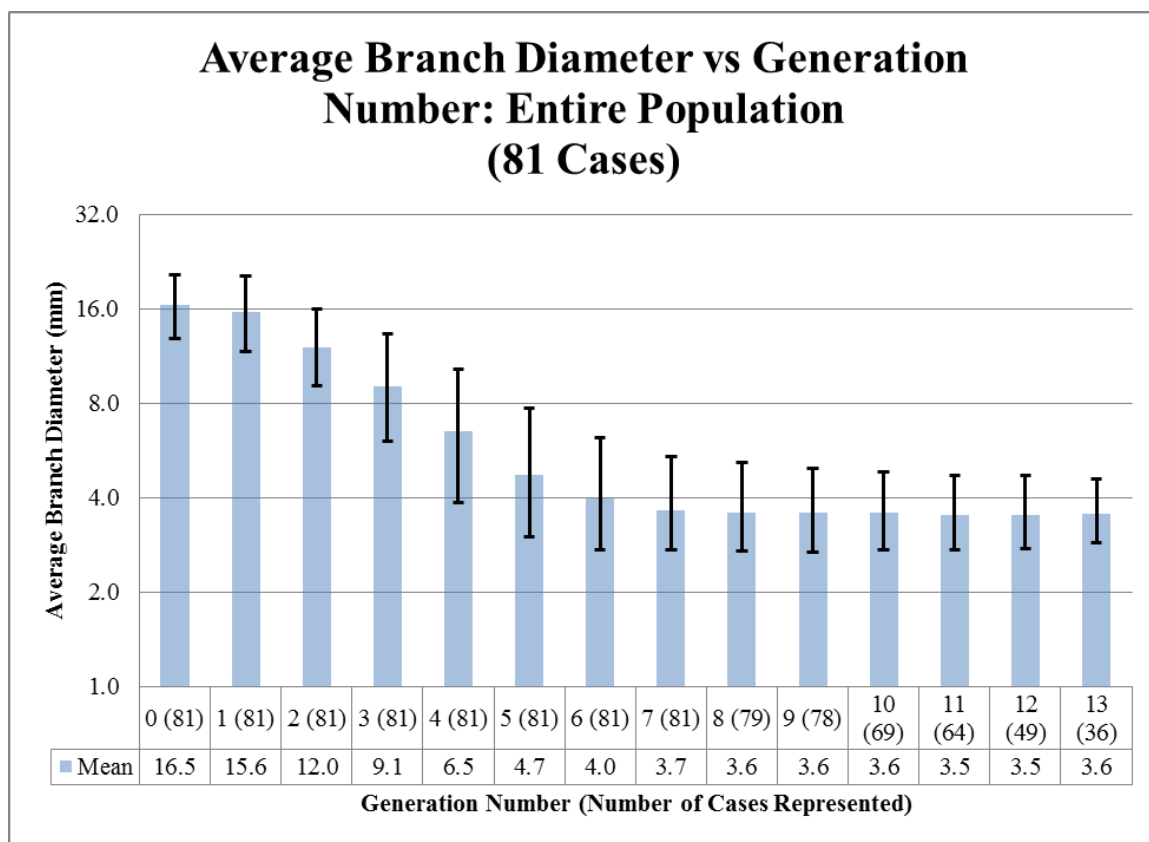


Figure 4.5: Average branch diameter vs. generation number for the entire population up to generation 13. The x-axis values represent the generation number. The number in parentheses represents the number of cases represented by that generation. Endpoints of the bars represent 5th and 95th percentiles. Note the y-axis is a logarithmic scale with base 2.

Global Airway Diameter Table						
Average Diameter vs. Generation						
	Our Study					Weibel
Generation (Number of Cases)	Number of Branches	95%	5%	Mean	σ	Weibel Diameter
0 (81)	81	20.6	12.8	16.5	2.4	18.0
1 (81)	162	20.3	11.6	15.6	2.6	12.2
a. Right Main Bronchus	81	20.8	13.6	17.0	2.4	
b. Left Main Bronchus	81	17.6	11.2	14.2	2.0	
2 (81)	322	16.0	9.1	12.0	2.1	8.3
3 (81)	638	13.3	6.0	9.1	2.3	5.6
4 (81)	1262	10.2	3.8	6.5	2.0	4.5
5 (81)	2374	7.7	3.0	4.7	1.4	3.5
6 (81)	3674	6.2	2.7	4.0	1.1	2.8
7 (81)	4230	5.4	2.7	3.7	0.9	2.3
8 (79)	3261	5.2	2.7	3.6	0.8	1.9
9 (78)	2030	5.0	2.7	3.6	0.7	1.5
10 (69)	1254	4.8	2.7	3.6	0.7	1.3
11 (64)	751	4.7	2.7	3.5	0.7	1.1
12 (49)	364	4.7	2.7	3.5	0.6	1.0
13 (36)	172	4.6	2.9	3.6	0.6	0.8
14 (19)	74	4.6	2.8	3.5	0.6	0.7
15 (9)	34	4.3	2.9	3.6	0.4	0.7
16 (3)	8	4.8	3.0	3.7	0.5	0.6
17 (1)	2	4.2	4.2	4.2	0.1	0.5
18 (1)	2	4.7	3.7	4.2	0.7	0.5
19 (1)	2	4.4	3.9	4.1	0.4	0.5
20 (1)	2	4.6	3.3	4.0	1.0	0.5
21 (1)	2	3.2	3.2	3.2	0.0	0.4
22 (1)	2	2.9	2.7	2.8	0.1	0.4

Table 4.1: Statistics for average branch diameter by generation for all generations. Right and left main bronchus data is listed separately beneath generation 1 data. Ewald Weibel's mean diameter findings are listed in the last column [1]. All measurements are in mm.

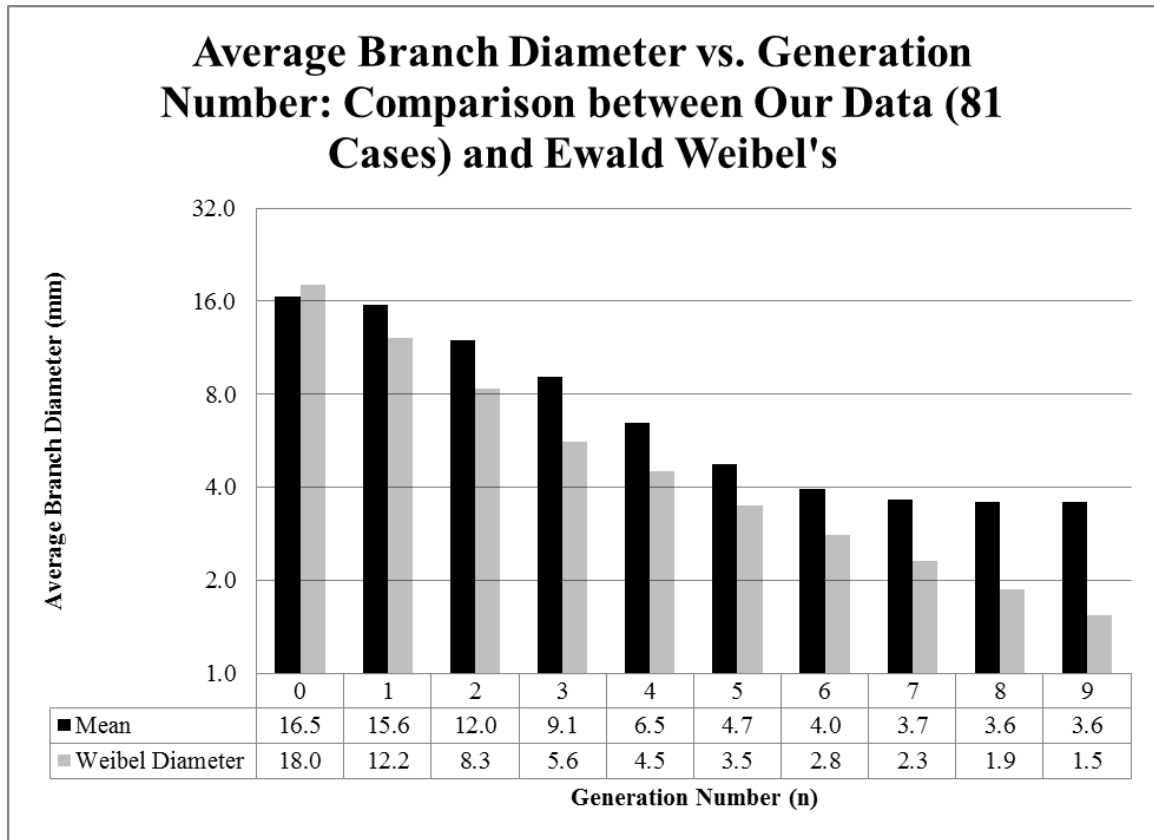


Figure 4.6: Comparison between the average diameter data generated by our study (black) and Weibel's calculations for an airway tree exhibiting a normal dichotomy (gray) [1]. Note the base 2 logarithmic scale.

We choose generation 13 as the cutoff point for the plot in Figure 4.5 as we lose 17 cases moving from generation 13 to generation 14, or 21% of the cases used in the study. This is the largest percentage drop for a single generation jump. We note that mean branch diameter decreases as generation increases. This is not unexpected, as each generation n contains approximately 2^n branches, as mentioned in Section 2.3. This necessitates that branch size decrease with an increase in generation number to accommodate the increased number of branches. This conclusion is supported by Weibel's calculations [1]. With exception of the trachea, our mean diameter numbers are larger than those calculated by Weibel. While the airway

tree does not exhibit a normal dichotomy, we still cite three potential sources for additional upward bias:

1. As mentioned in Section 1.2, the MIPL's segmentation software uses a conservative segmentation algorithm [6]. As such, many of the smaller branches are discounted, especially at higher generation numbers. As a result, the mean is skewed higher than is anatomically accurate. This may explain the growing discrepancy between our data and Weibel's as generation number increases.
2. Weibel's data is based on the study of five patients, ranging in age from 8 to 74 years old [1]. Our data uses only adult patients, and contains 81 cases. Additionally, Weibel used manual microscopic and macroscopic techniques to study dead tissue, while our data uses sub-millimeter resolution CT images taken from live patients.
3. Weibel's study was published in 1963. A rise in the average size of humans over the past 50 years may explain inflated numbers.

We also observe average branch diameter by lobar generation number, as defined in Section 3.2.2. This data is represented in Figure 4.7 and Table 4.2.

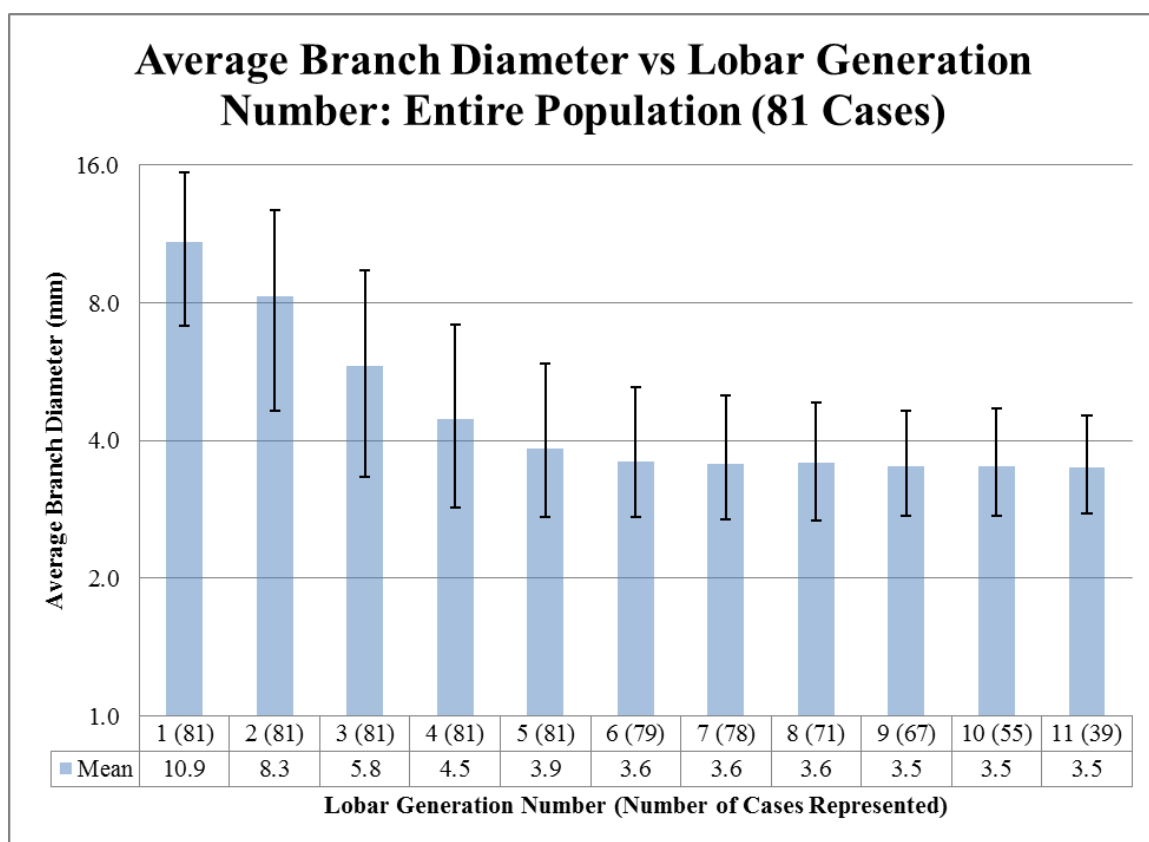


Figure 4.7: Average branch diameter vs. lobar generation number for the entire population up to lobar generation 11. The x-axis values represent the lobar generation number. The number in parentheses represents the number of cases with branches in that generation. Bars represent 5th and 95th percentiles.

Global Airway Diameter Table						
Average Diameter vs. Lobar Generation						
Lobar Generation (Number of Cases)	Number of Branches	95%	5%	Mean	σ	
1 (81)	401	15.4	7.1	10.9	2.5	
2 (81)	778	12.7	4.7	8.3	2.5	
3 (81)	1507	9.5	3.3	5.8	1.9	
4 (81)	2722	7.2	2.9	4.5	1.3	
5 (81)	3904	5.9	2.7	3.9	1.0	
6 (79)	4118	5.3	2.7	3.6	0.8	
7 (78)	2978	5.0	2.7	3.6	0.7	
8 (71)	1775	4.9	2.7	3.6	0.7	
9 (67)	1041	4.7	2.7	3.5	0.6	
10 (55)	540	4.7	2.7	3.5	0.6	
11 (39)	228	4.5	2.8	3.5	0.5	
12 (19)	82	4.6	2.8	3.5	0.6	
13 (10)	39	4.2	2.9	3.5	0.4	
14 (4)	8	3.9	3.0	3.4	0.3	
15 (1)	4	4.8	3.0	3.8	0.8	
16 (1)	2	4.2	4.2	4.2	0.1	
17 (1)	2	4.7	3.7	4.2	0.7	
18 (1)	2	4.4	3.9	4.1	0.4	
19 (1)	2	4.6	3.3	4.0	1.0	
20 (1)	2	3.2	3.2	3.2	0.0	
21 (1)	2	2.9	2.7	2.8	0.1	

Table 4.2: Statistics for average branch diameter by lobar generation for all lobar generations. All measurements are in mm.

Lobar generation provides a more like-to-like comparison of branches, as explained in Section 3.2.2. As was the case in Figure 4.5 with generation number, we limit the number of lobar generations displayed in the plot in Figure 4.7. As demonstrated in Table 4.2, the jump from lobar generation 11 to lobar generation 12 results in the loss of 20 cases, or roughly 25% of the entire population. Also similar to the raw generation data, the mean branch diameter decreases as lobar generation number increases.

In addition to observing branch diameters, we are interested in viewing trends in branch lengths. Figure 4.8 contains a plot of branch lengths by generation number for the first 13 generations after the trachea. Table 4.3 contains branch length statistics for all generations present in the analysis. Figure 4.9 compares our branch length measurements to Weibel's calculations.

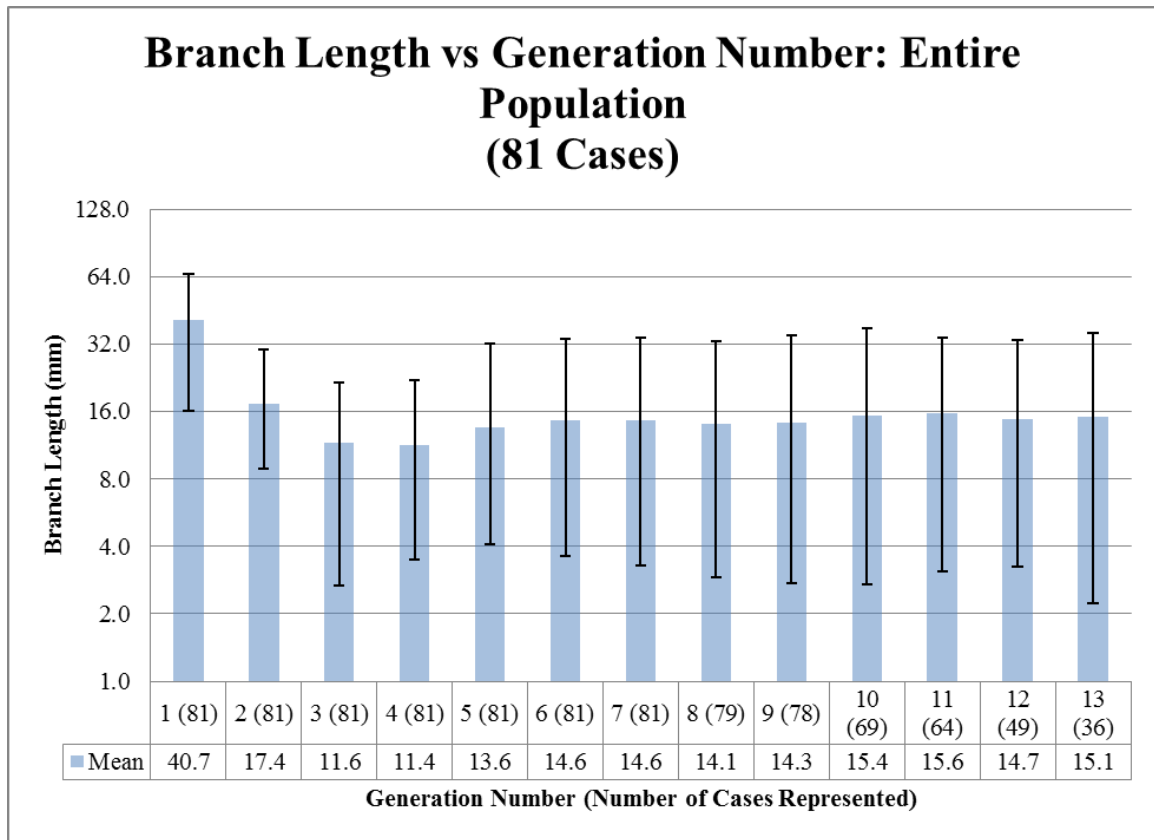


Figure 4.8: Average branch diameter vs. generation number for the entire population up to generation 13 excluding the trachea. The trachea's starting point is arbitrarily defined in the MIPL software, rendering length data unreliable. The x-axis values represent the generation number. The number in parentheses represents the number of cases represented by that generation. Bars represent 5th and 95th percentiles. Note the y axis is a base 2 logarithmic scale.

Global Airway Length Table						
Branch Length vs. Generation						
	Our Study					Weibel
Generation(Number of Cases)	Number of Branches	95%	5%	Mean	σ	Weibel Length
0 (81)	81	124.3	81.3	101.8	12.4	120.0
1 (81)	162	65.9	16.1	40.7	16.5	47.6
a. Right Main Bronchus	81	41.0	15.3	26.1	6.9	
b. Left Main Bronchus	81	68.1	44.4	55.4	5.9	
2 (81)	322	30.2	8.9	17.4	6.9	19.0
3 (81)	638	21.6	2.7	11.6	9.3	7.6
4 (81)	1262	22.0	3.5	11.4	10.3	12.7
5 (81)	2374	32.1	4.1	13.6	10.1	10.7
6 (81)	3674	33.9	3.6	14.6	9.7	9.0
7 (81)	4230	34.3	3.3	14.6	10.3	7.6
8 (79)	3261	32.8	2.9	14.1	10.9	6.4
9 (78)	2030	35.0	2.8	14.3	10.3	5.4
10 (69)	1254	37.6	2.7	15.4	9.7	4.6
11 (64)	751	34.1	3.1	15.6	10.5	3.9
12 (49)	364	33.1	3.3	14.7	12.5	3.3
13 (36)	172	35.8	2.2	15.1	11.1	2.7
14 (19)	74	43.0	2.2	15.8	6.7	2.3
15 (9)	34	31.0	1.3	14.7	0.9	2.0
16 (3)	8	18.7	1.4	7.7	0.2	1.7
17 (1)	2	3.1	1.8	2.4	2.1	1.4
18 (1)	2	3.0	2.7	2.8	1.0	1.2
19 (1)	2	3.8	0.8	2.3	14.1	1.0
20 (1)	2	3.8	2.4	3.1	8.6	0.8
21 (1)	2	23.3	3.4	13.4	6.0	0.7
22 (1)	2	16.8	4.6	10.7	5.2	0.6

Table 4.3: Statistics for branch length by generation for all generations. Right and left main bronchus data is listed separately beneath generation 1 data. Ewald Weibel's mean branch length calculations are listed in the last column [1]. All measurements are in mm.

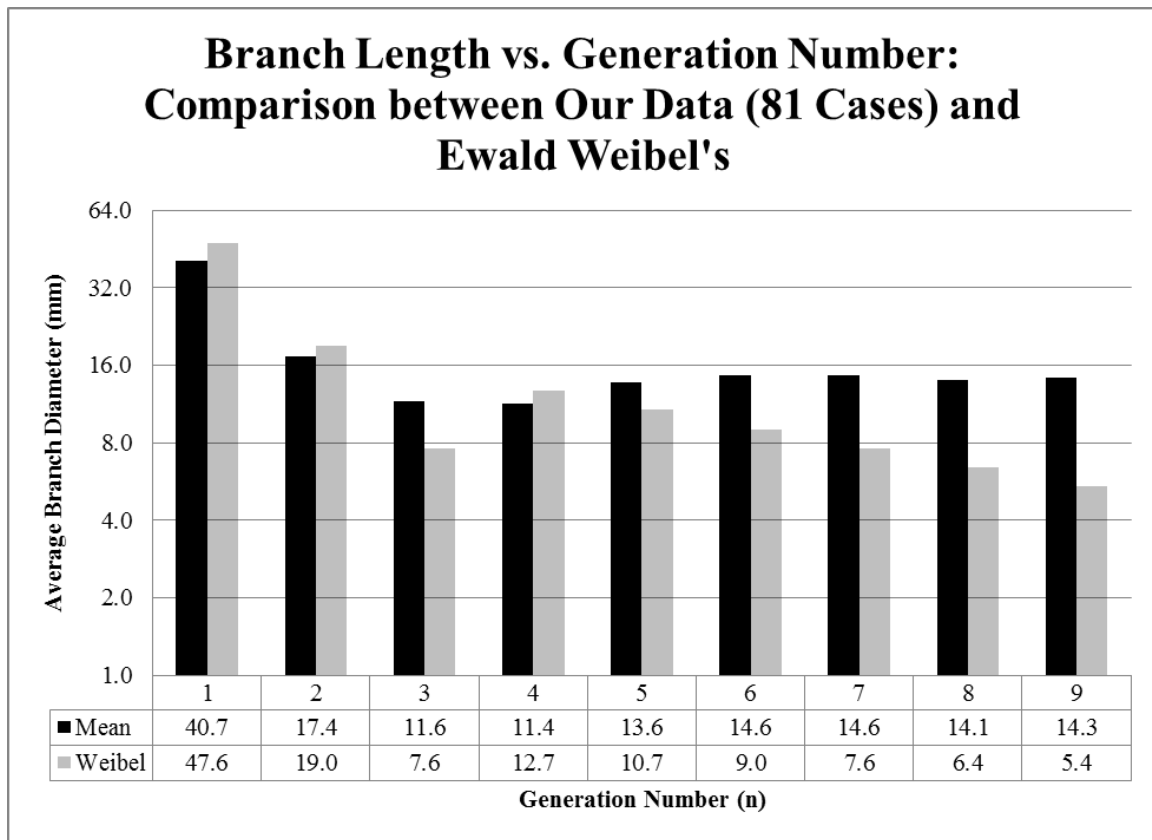


Figure 4.9: Comparison between branch length the data generated by our study (black) and Weibel's calculations (gray) [1]. Note the base 2 logarithmic scale.

We limited the horizontal axis of the plots in Figures 4.8 and 4.9 for the same reasons given for Figures 4.5 and 4.6. Unlike with average diameter, mean branch length does not decrease for every increase in generation. Figure 4.8 shows that for our data, generation 3 and 4 branches were the shortest on average until generation 16, which represents just three of the 81 cases. Weibel's data partially supports this trend, yet in his study, generation 4 is the only generation to show a higher mean than the previous generation. This is in contrast to ours, in which generations 5 and 6, among others, show an increase over the previous generation. Sources of contrast are likely the same as with average branch diameter.

As was the case with average branch diameter, we look at branch lengths by lobar generation number. Figure 4.10 gives a plot of branch length by lobar generation, while Table 4.4 gives additional statistics in tabular format.

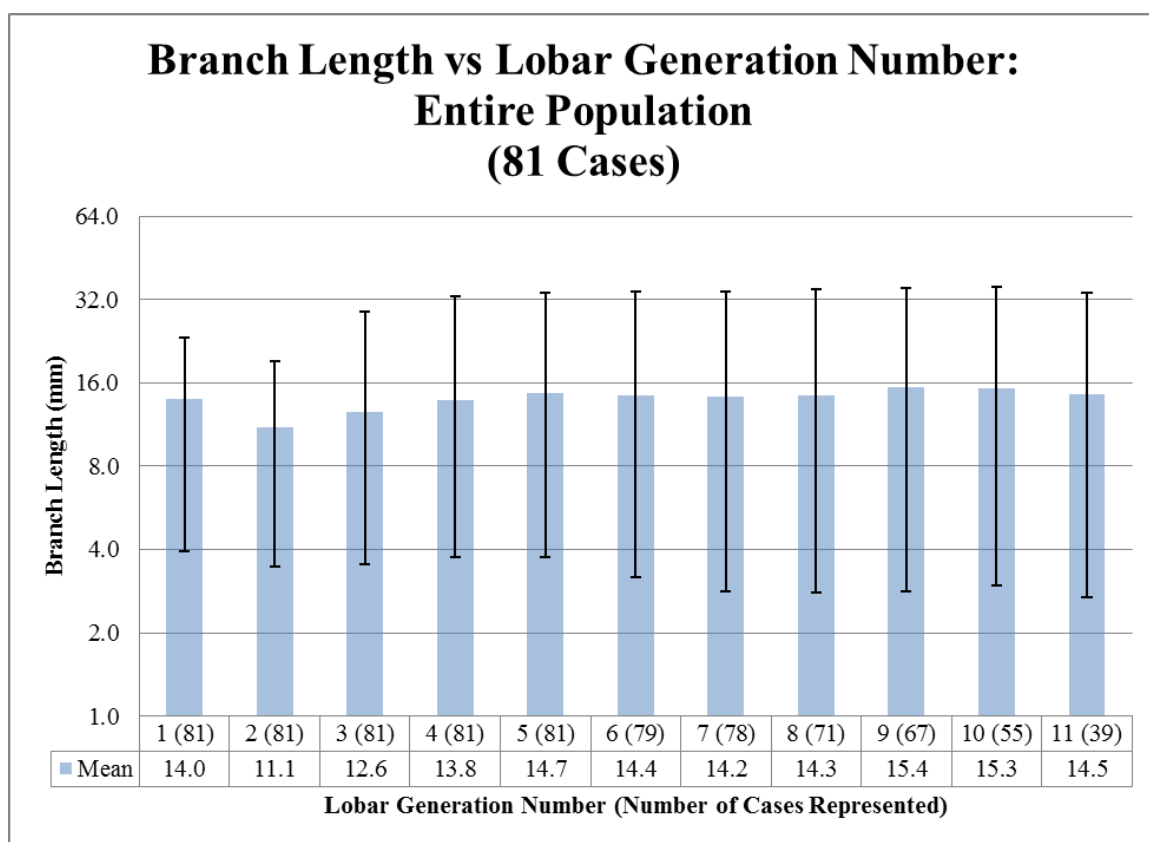


Figure 4.10: Branch length vs. lobar generation number for the entire population up to lobar generation 11. The x-axis values represent the lobar generation number. The number in parentheses represents the number of cases with branches in that lobar generation. Bars represent 5th and 95th percentiles.

Global Airway Length Table					
Branch Length vs. Lobar Generation					
Lobar Generation (Number of Cases)	Number of Branches	95%	5%	Mean	σ
1 (81)	401	23.4	4.0	14.0	6.0
2 (81)	778	19.1	3.5	11.1	5.2
3 (81)	1507	28.8	3.5	12.6	8.9
4 (81)	2722	32.8	3.8	13.8	9.5
5 (81)	3904	33.8	3.8	14.7	10.2
6 (79)	4118	34.1	3.2	14.4	10.0
7 (78)	2978	34.2	2.8	14.2	9.9
8 (71)	1775	34.9	2.8	14.3	10.3
9 (67)	1041	35.3	2.8	15.4	10.6
10 (55)	540	35.5	3.0	15.3	10.3
11 (39)	228	33.8	2.7	14.5	10.0
12 (19)	82	42.2	2.1	15.5	12.4
13 (10)	39	32.2	1.4	15.2	10.6
14 (4)	8	18.7	0.3	7.3	7.0
15 (1)	4	4.3	1.4	3.2	1.3
16 (1)	2	3.1	1.8	2.4	0.9
17 (1)	2	3.0	2.7	2.8	0.2
18 (1)	2	3.8	0.8	2.3	2.1
19 (1)	2	3.8	2.4	3.1	1.0
20 (1)	2	23.3	3.4	13.4	14.1
21 (1)	2	16.8	4.6	10.7	8.6

Table 4.4: Statistics for branch length by lobar generation for all lobar generations. All measurements are in mm.

Based on our data, branch length remains relatively consistent as lobar generation is increased. This is likely due to the segmentation software discounting smaller branches in the segmentation, as explained in Section 1.2. This may be particularly problematic for branch length, as discounting a daughter branch of branch n results in no bifurcation, so the segmentation software considers branch n and its one daughter as the same branch, resulting in a branch that is effectively twice as long.

We also consider angle with parent branch in our study. We observe a similarity between the 3-point and 5-point angle with parent measurements. As such, we omit the 5-point angle with parent measurement from our plots and tables. Accordingly, all displayed data reflects the 3-point angle with parent. Branch angle data by generation is illustrated in Figure 4.11 and Table 4.5. Branch angle data by lobar generation is illustrated in Figure 4.12 and Table 4.6.

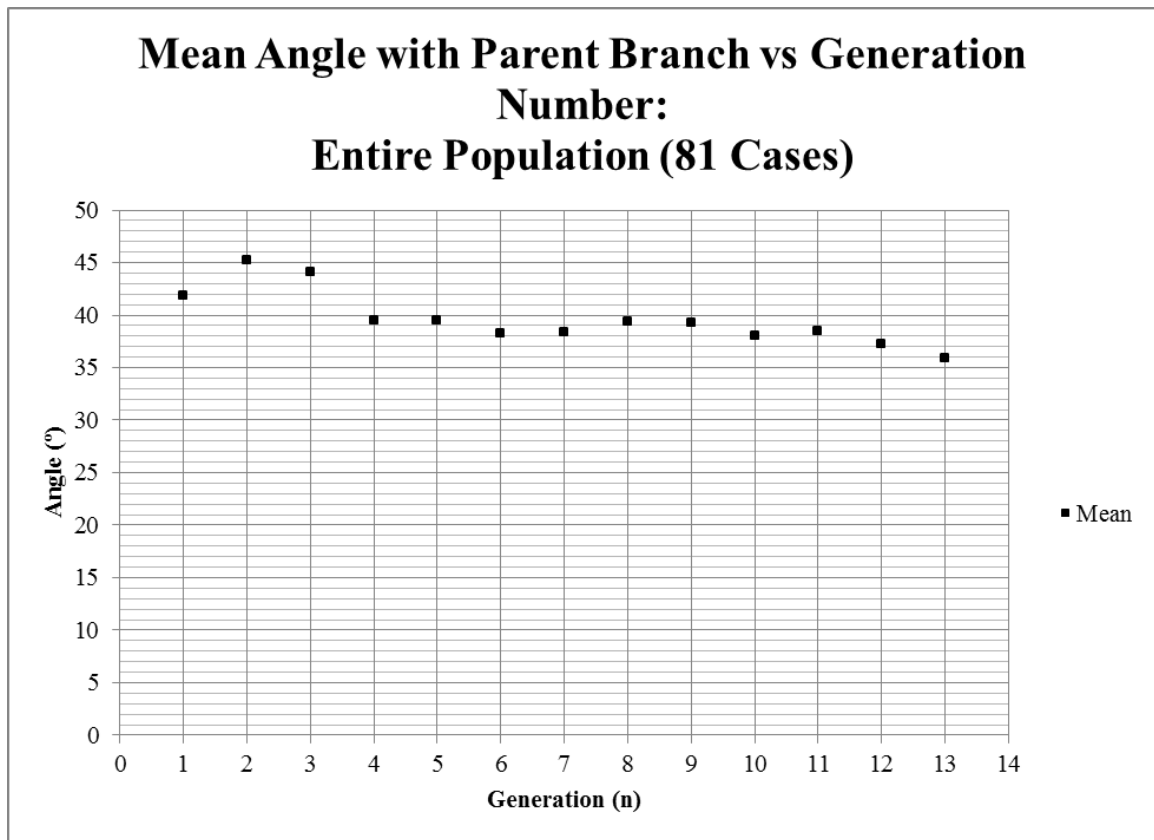


Figure 4.11: Mean angle with parent branch vs. generation number. Note only data up to generation 13 is displayed in the plot.

Global Angle with Parent Table								
Angle with Parent vs. Generation								
Generation (Number of Cases)	Number of Branches	Mean	Median	Maximum	Minimum	σ	5%	95%
0 (81)	81	0	0	0	0	0	0	0
1 (81)	162	42	38	119	14	19	19	75
2 (81)	322	45	42	130	1	22	12	85
3 (81)	638	44	42	161	1	25	7	88
4 (81)	1262	40	37	174	0	23	7	77
5 (81)	2374	39	37	178	0	22	10	77
6 (81)	3674	38	36	168	0	20	10	72
7 (81)	4230	38	35	178	0	21	11	73
8 (79)	3261	39	36	178	1	22	11	76
9 (78)	2030	39	36	175	0	21	11	75
10 (69)	1254	38	36	178	1	21	10	73
11 (64)	751	38	37	178	0	21	9	71
12 (49)	364	37	36	122	1	20	10	71
13 (36)	172	36	31	121	2	21	9	78
14 (19)	74	37	33	89	3	20	7	71
15 (9)	34	42	38	109	1	22	18	87
16 (3)	8	46	46	81	21	23	21	81
17 (1)	2	50	50	98	2	68	2	98
18 (1)	2	56	56	108	5	73	5	108
19 (1)	2	47	47	67	28	27	28	67
20 (1)	2	47	47	89	5	59	5	89
21 (1)	2	90	90	168	11	111	11	168
22 (1)	2	43	43	54	33	15	33	54

Table 4.5: Table of angle with parent statistics by generation for all cases.

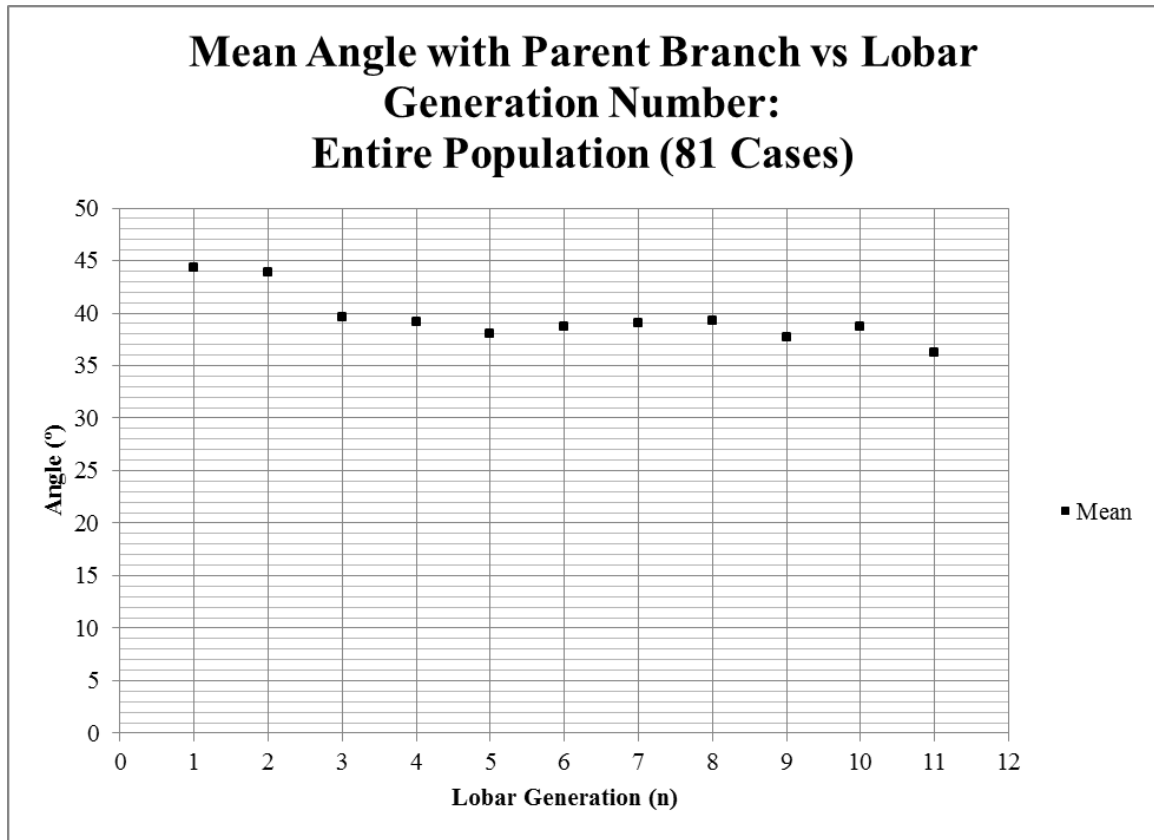


Figure 4.12: Angle with parent vs. lobar generation number. Note only up to lobar generation 11 is displayed in the plot.

Global Angle with Parent Table								
Angle with Parent vs. Lobar Generation								
Lobar Generation (Number of Cases)	Number of Branches	Mean	Median	Maximum	Minimum	σ	5%	95%
1 (81)	401	44	42	135	1	23	7	86
2 (81)	778	44	42	161	1	24	7	87
3 (81)	1507	40	37	174	0	23	8	77
4 (81)	2722	39	37	178	0	21	9	76
5 (81)	3904	38	36	178	0	20	11	71
6 (79)	4118	39	36	176	0	21	11	73
7 (78)	2978	39	36	178	0	21	11	76
8 (71)	1775	39	36	178	1	21	11	75
9 (67)	1041	38	36	175	0	21	9	71
10 (55)	540	39	37	178	1	21	9	74
11 (39)	228	36	32	121	2	20	10	72
12 (19)	82	36	33	87	3	19	8	71
13 (10)	39	40	38	89	3	20	10	84
14 (4)	8	45	30	109	1	37	1	109
15 (1)	4	55	57	71	36	14	36	71
16 (1)	2	50	50	98	2	68	2	98
17 (1)	2	56	56	108	5	73	5	108
18 (1)	2	47	47	67	28	27	28	67
19 (1)	2	47	47	89	5	59	5	89
20 (1)	2	90	90	168	11	111	11	168
21 (1)	2	43	43	54	33	15	33	54

Table 4.6: Table of angle with parent statistics by lobar generation.

The mean angle with parent branch is relatively consistent across all generations and lobar generations. We note, however, that some branches have angles near 180° and 0 , a case which is not practical in normal anatomical instances. These extreme angles are due to anomalies in the segmentations of the trees in question. In these cases, the branch centerline as defined by the MIPL software takes off at a locally (several viewsites) extreme angle, then curves to a more standard direction. This case is illustrated in Figure 4.13.

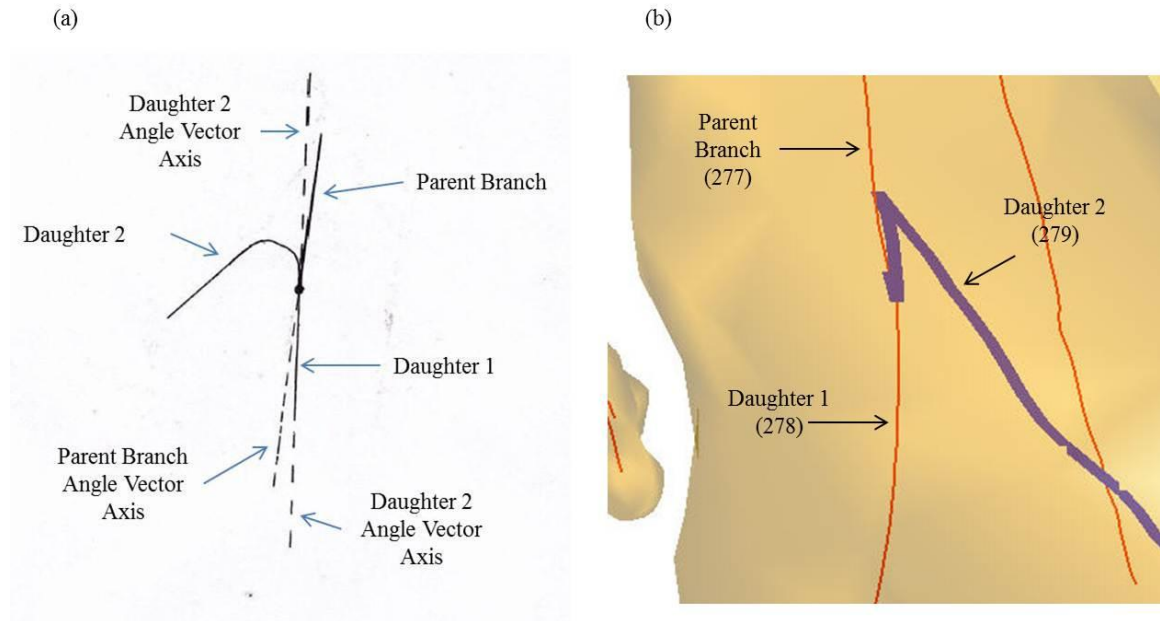


Figure 4.13: (a) Illustration of extreme (near 180° or 0°) branch angles. Angle vector axes (AVAs, dashed lines) are extensions of vectors made from distal three (parent) or proximal three (daughter) viewsites. The angle between the parent AVA and daughter 1 AVA is near 180° while the angle between the parent AVA and daughter 1 AVA is near 0. (b) Extreme angle in case 21405_12. Branch 279 (centerline in blue) leaves at approximately 175°.

For this reason, the angle with parent measurements are less reliable than those involving branch diameters and lengths.

We also observe average branch diameter in each lobe, shown in Figure 4.14.

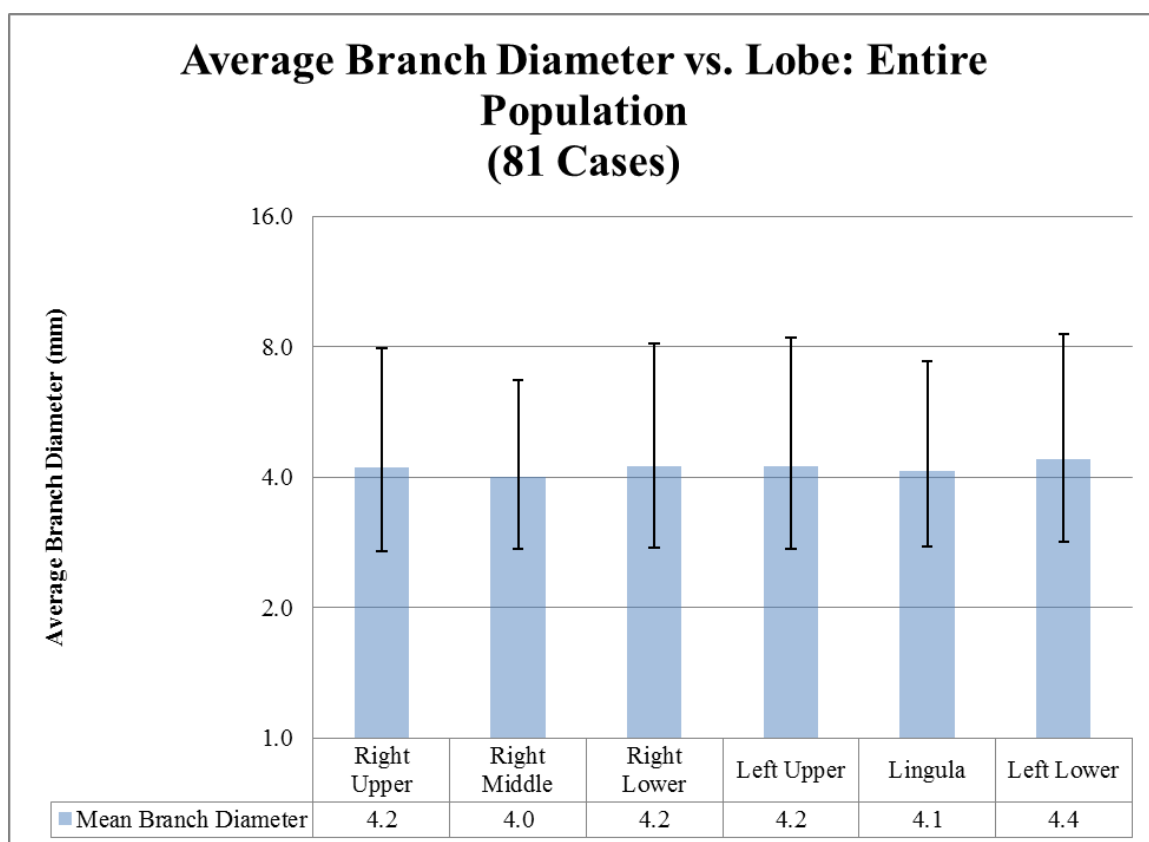


Figure 4.14: Average branch diameters by lobe. Columns represent the mean diameters. Bars represent the 5th and 95th percentiles. Note each lobe contains a range of generations, contributing to the large range of diameters in each lobe.

As illustrated in Figure 4.14, there is not a large difference in mean branch diameter from one lobe to another. We note, however, that the left lower lobe contains the largest branches, while the left upper, right lower, and right upper lobes contain approximately the same size branches, just smaller than the left lower lobe. The lingula and right middle lobe contain the smallest branches on average.

4.2.2: Analysis by Gender

Section 4.2.2 provides a comparison of branch diameter and branch length by gender.

Average branch diameter is plotted against lobar generation number for both genders in Figure 4.15. Branch length is plotted against lobar generation number for both genders in Figure 4.16.

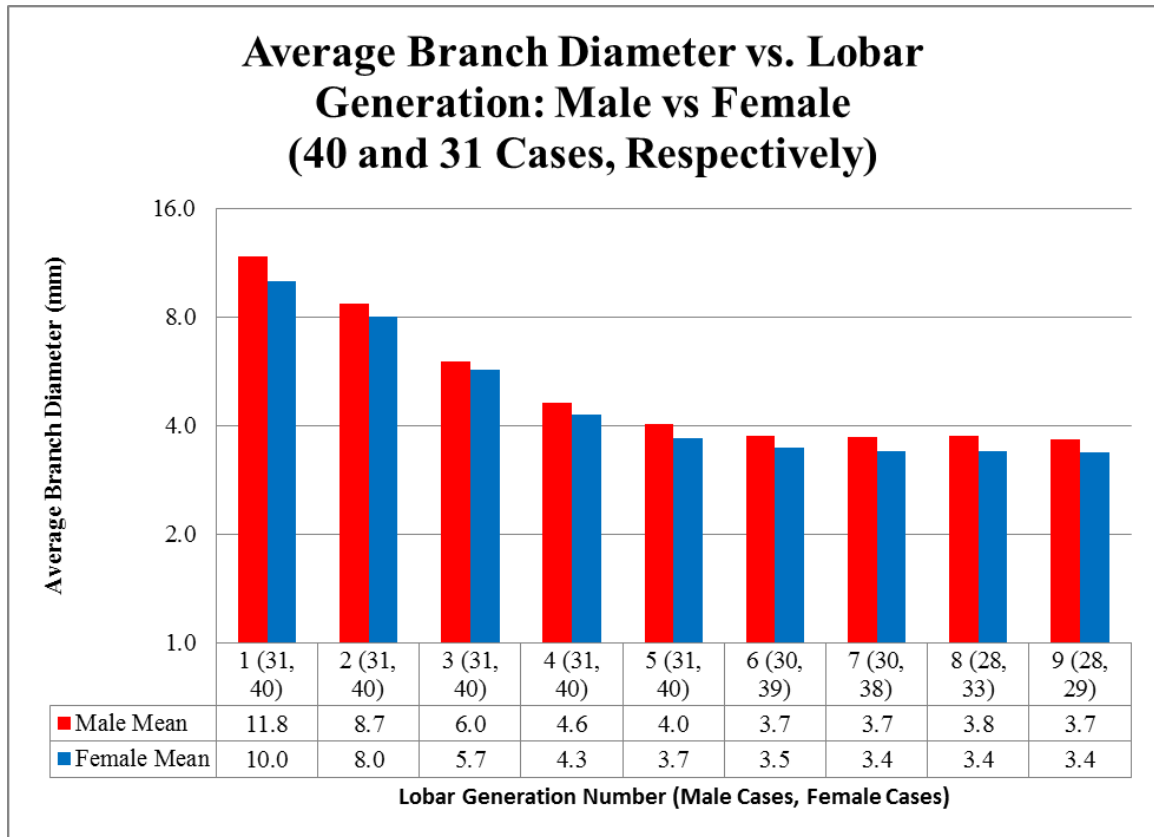


Figure 4.15: Mean average branch diameter vs. lobar generation for both males and females. The numbers in parentheses represent the number of cases containing branches in that generation for each gender (male, female). Note the base 2 logarithmic y-axis scale.

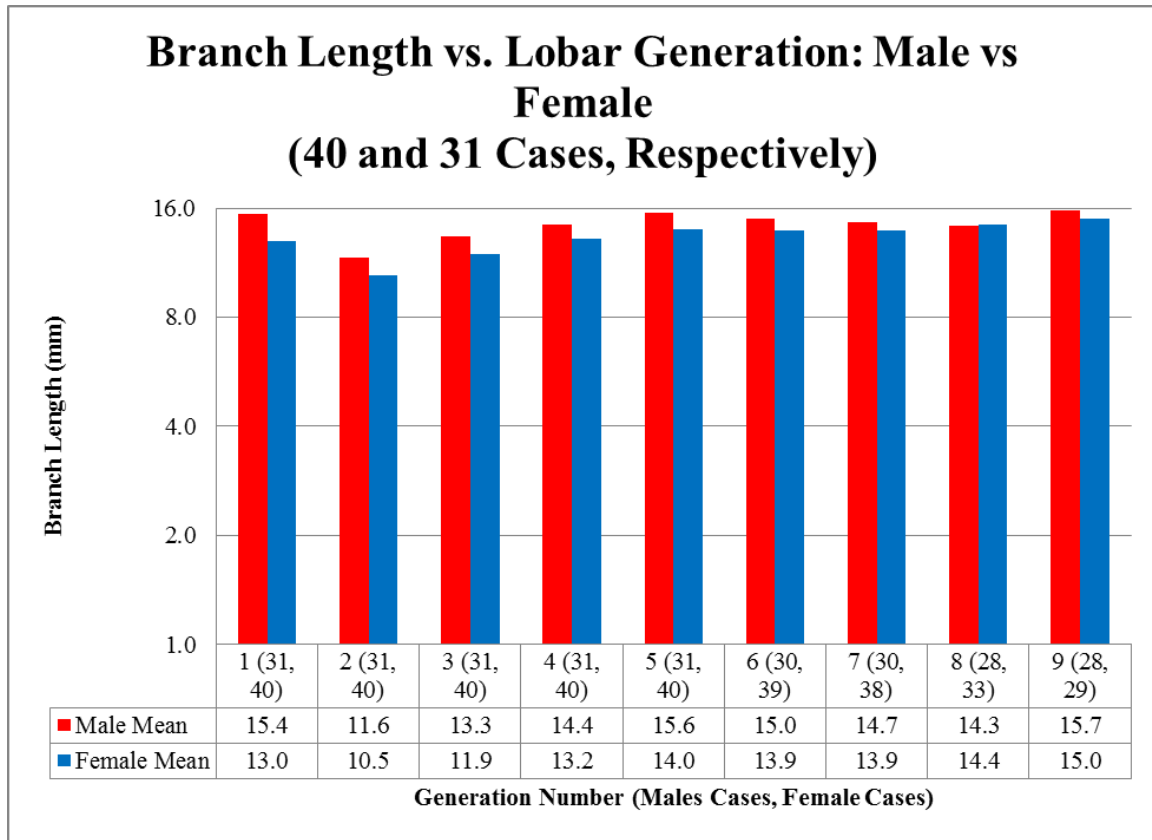


Figure 4.16: Mean branch length vs. lobar generation for both males and females. The numbers in parentheses represent the number of cases containing branches in that generation for each gender (male, female). Note the base 2 logarithmic y-axis scale.

Based on this data, the average male branch is larger than a comparable female branch. It is unclear from our data whether this is simply because males are, on average, larger than females, or if a comparably-sized male and female have comparably-sized branches.

4.2.3: Analysis by BMI

Section 4.2.3 provides a comparison of average branch diameters among the four BMI characterizations as defined by the World Health Organization [9]. Figure 4.17 plots average branch diameter by lobar generation for these four categories.

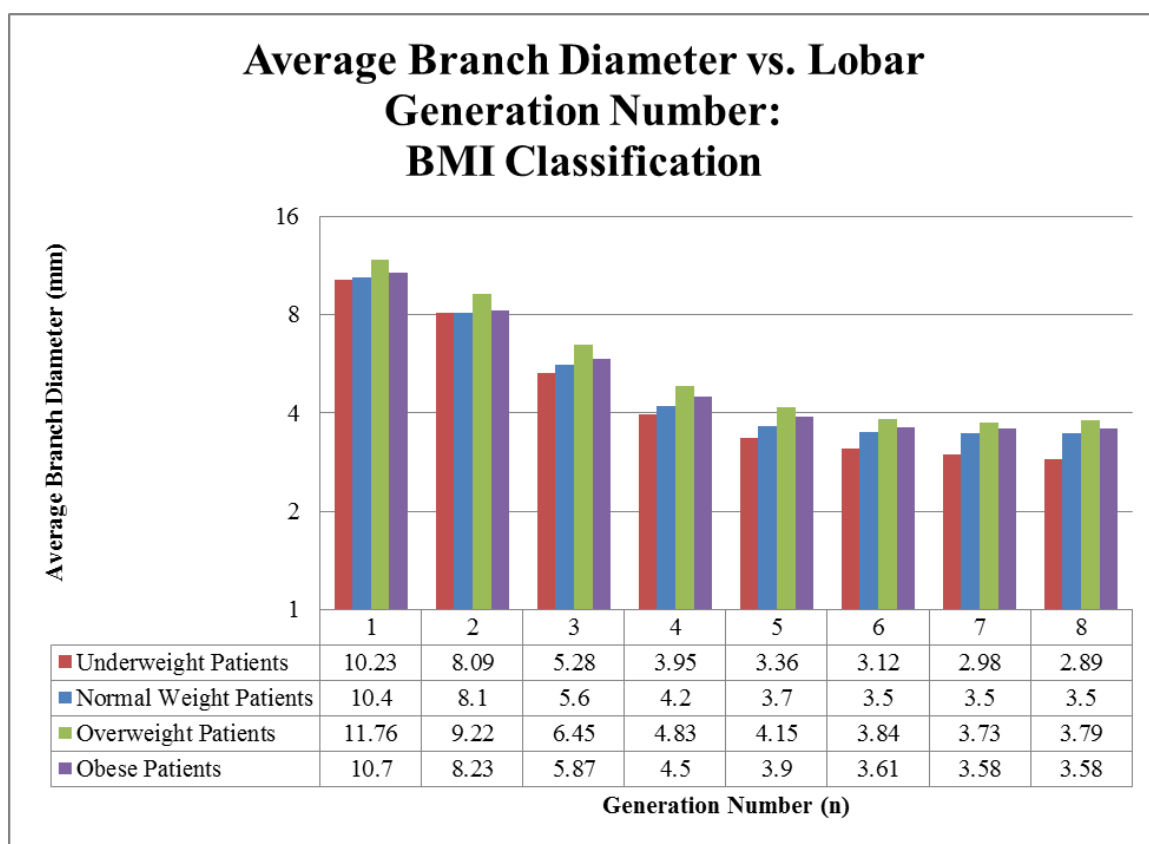


Figure 4.17: Average branch diameter vs. lobar generation number for all four BMI classifications. Note the base 2 logarithmic y-axis scale.

Figure 4.17 demonstrates that mean branch diameter increases with BMI, with the exception of obese cases. This indicates that for a given height, a heavier patient will have wider airways with the maximum occurring at an overweight ratio. Obese-patient branches may be narrowed due to health-related occlusion, though this is unclear from our data.

Chapter 5

Discussion and Future Work

Section 5.1 outlines general conclusions we have drawn from our study. Section 5.2 discusses potential future directions.

5.1: Conclusions

- Airway diameter decreases with generation.
- Males tend to have larger airways than females.
- Branch diameter increases with weight, reaching a maximum at an overweight BMI.
- As Weibel concludes, statistics vary from those expected in a regular dichotomy.
- Statistics by lobar generation provide a more like-to-like analysis, as the standard deviation is lower than for a raw generation (albeit slightly).

5.2: Future Directions

The MIPL has done significant work in the fields of 3D medical image processing and navigational bronchoscopy. A thorough quantitative analysis of the airway tree using high resolution MDCT has the potential to help improve strategies used in navigational bronchoscopy and to help improve image processing techniques by highlighting anomalies. While our study provides useful comparisons among different branch populations, there are several ways in which the study may be improved upon in the future.

- *Create a more robust C++ program.* The BranchStats code was not designed to be as robust as possible due to the multitude of anatomical variations and our ability to manually edit the BranchData file. In several cases (Appendix A), BranchStats incorrectly identified which of two conjugate key branches (as explained in Section 3.2.2) was which. This required manual inspection followed by manual editing to create an accurate BranchData file. For example, a better method for deciding between the right middle lobe parent and right upper lobe parent could be devised, as this decision point failed in several cases (Appendix A). In other cases not included in the study, certain anatomical variations rendered identification techniques obsolete or caused BranchStats to terminate without creating a BranchData file. To account for all variations would have taken significantly longer and is outside of the scope of our study.
- *Identify more key branches.* While the lobar bronchi (lobe parents) allow us to view the lobes as aggregates, previous studies have identified and performed analysis more distal branches [4]. This would allow for a more focused understanding of particular branches within the lung, which may help identify problems with current bronchoscopic techniques.
- *Compare with similar mammalian airway trees.* Merryn Tawhai's 2004 study compares the human airway with the ovine (sheep) airway tree [5]. It may be of interest to compare the human airway tree to those of primates, bovine (cows), and other mammals.

Appendix A

Cases Used

Appendix A contains information on the database of cases used in our study. All data used in our study is contained within the folder “\\carew\Z\mra5101\MikeWork.” All case studies are stored in the folder \\carew\Z\mra5101\MikeWork\Thesis Cases. All Analysis files are stored in the folder “\\carew\Z\mra5101\MikeWork\Compilation Files.” Table A.1 lists all cases identified only by Penn State Hershey Medical Center (PSHMC) IRB protocol number. Along with protocol number, the number of branches, highest generation and lobar generation present in the case, gender, BMI classification, images used in reconstruction, and supplemental notes are displayed in columns across the table. Table A.2 contains the 3D renderings of all airway trees used in our study. Each rendering is identified by its PSHMC IRB protocol number.

Cases Used in Our Study							
Case Number	Number of Branches	Max Generation	Max Lobar Generation	Gender	BMI Category	Kernels Used	Notes
20349_3_1	243	14	12	Unknown	Unknown	B30, B50	1
20349_3_2	313	12	10	Unknown	Unknown	B30, B50	2
20349_3_6	347	13	11	Unknown	Unknown	B31, B50	
20349_3_9	203	11	9	Unknown	Unknown	B31, B50	
20349_3_11	305	13	11	Unknown	Unknown	B31, B50	2
20349_3_12	193	11	9	Unknown	Unknown	B31, B50	3
20349_3_13	367	12	11	Unknown	Unknown	B31, B50	

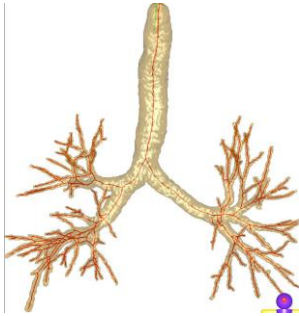
20349_3_14	161	11	9	Unknown	Unknown	B31, B50	
20349_3_15	427	15	13	Unknown	Unknown	B31, B50	3
20349_3_16	323	13	11	Unknown	Unknown	B31, B50	4
20349_3_17	197	11	9	F	Normal	B31, B50	2
20349_3_19	349	13	11	M	Unknown	B31, B50	
20349_3_20	127	10	8	F	Normal	B31, B50	
20349_3_21	209	11	9	F	Obese	B31, B50	
20349_3_22	51	8	6	F	Unknown	B41	9
20349_3_23	365	13	11	M	Obese	B50	
20349_3_24	277	14	12	F	Overweight	B31, B50	
20349_3_25	285	11	10	M	Obese	B31, B70	
20349_3_26	163	9	8	F	Underweight	B31, B50	
20349_3_27	219	14	12	M	Overweight	B31, B50	
20349_3_28	125	10	9	F	Normal	B31, B50	2
20349_3_29	153	9	8	F	Normal	B31, B50	
20349_3_30	291	13	11	F	Normal	B31, B50	
20349_3_31	355	14	12	M	Obese	B31, B50	
20349_3_32	441	13	11	F	Overweight	B31, B50	
20349_3_33	333	14	13	M	Overweight	B31, B50	2
20349_3_34	295	12	10	M	Obese	B31, B50	
20349_3_35	123	11	9	F	Obese	B31, B50	2
20349_3_36	281	14	12	M	Obese	B31, B50	
20349_3_37	125	9	7	F	Unknown	B31, B50	2
20349_3_38	217	13	11	F	Normal	B31, B50	

20349_3_39	271	14	12 F	Normal	B31, B50	
20349_3_40	245	12	10 F	Underweight	B31, B50	5
20349_3_41	301	15	13 F	Obese	B31, B50	2
20349_3_43	55	7	5 M	Unknown	B30, B50	9
20349_3_45	73	9	7 M	Obese	B31, B50	9
20349_3_46	257	12	10 F	Obese	B31, B50	
20349_3_47	221	11	9 F	Unknown	B30, B50	
20349_3_49	275	11	10 M	Obese	B30, B50	
20349_3_50	428	22	21 F	Unknown	B31, B50	
20349_3_51	590	15	14 F	Normal	B30, B50	
20349_3_52	41	7	5 F	Unknown	B30, B50	4, 9
20349_3_53	147	10	8 F	Normal	B30, B50	4
20349_3_55	191	11	10 M	Unknown	B80	
20349_3_56	139	9	7 M	Normal	B30, B50	
20349_3_57	99	9	7 F	Unknown	PET/CT	6
20349_3_58	375	16	14 M	Unknown	B31, B50	
20349_3_59	363	13	11 M	Unknown	B31, B50	
20349_3_61	189	12	11 F	Overweight	B31, B80	
20349_3_62	223	11	10 M	Obese	B31, B50	
20349_3_64	431	15	13 M	Overweight	B31, B50	
20349_3_66	227	13	11 F	Overweight	B31, B50	
20349_3_67	223	11	10 M	Obese	B31	2
20349_3_68	251	14	12 F	Obese	B70	
20349_3_69	307	13	11 F	Obese	B30, B50	

21405_12	287	13	11 M	Overweight	B30, B50	
21405_19	57	10	9 M	Obese	B30, B50	9
21405_20	197	10	9 F	Underweight	B30, B50	2, 7
21405_22	115	11	9 M	Obese	B30, B50	
21405_57	99	9	7 F	Obese	B31, B50	
21405_59	363	13	11 M	Normal	B31, B50	4
21405_60	189	13	11 F	Obese	B31, B50	
21405_63	311	12	10 F	Obese	B25, B50	
21405_64	365	14	12 F	Obese	B31, B50	
21405_66	151	9	7 F	Normal	B31, B50	2
21405_67	357	15	13 M	Normal	B31, B50	
21405_69	45	9	7 F	Normal	B31, B50	9
21405_70	299	12	11 F	Unknown	B31, B50	
21405_72	483	13	11 M	Overweight	B31, B50	
21405_73	289	12	10 M	Obese	B31, B50	
21405_74	243	12	10 F	Obese	B31, B50	
21405_75	227	12	10 M	Unknown	B31, B50	8
21405_77	483	15	13 M	Overweight	B31, B50	
21405_78	179	11	9 F	Normal	B31, B50	
21405_80	228	12	10 M	Overweight	B31, B50	2
21405_91	267	14	12 M	Overweight	B50	
21405_92	229	11	10 F	Unknown	B31, B50	2
21405_93	373	13	11 F	Normal	B31, B50	
21405_95	251	12	10 M	Obese	B31, B50	4

21405_96	513	16	14	M	Overweight	B50	
21405_97	217	13	11	F	Normal	B31, B50	
1: BranchStats did not identify lingula parent or lingula branches. These were identified by manually editing the text file.							
2: BranchStats did not correctly identify right middle lobe parent and right lower lobe parent; RML was labeled as RLL and vice versa. As such, all RML and RLL branches were incorrectly categorized. This was fixed by manually editing the text file.							
3: Right intermediary bronchus daughters exhibited abnormal geometry, explained in section 4.1.							
4: C++ did not assign lobar values for right middle and right lower lobes. Assignments were made by manually editing the text file.							
5: The right middle lobe of this tree consisted only of the right middle lobe parent branch.							
6: PET/CT Scan used							
7: C++ did not assign lobar values for left upper and left lower lobes. Assignments were made by manually editing the text file.							
8: BranchStats did not correctly identify left upper lobe parent and left lower lobe parent; LUL was labeled as LLL and vice versa. As such, all LUL and LLL branches were incorrectly categorized. This was fixed by manually editing the text file.							
9: Indicates sparse tree, likely due to a noisy image or airway obstruction.							

Table A.1: Cases used in our study.

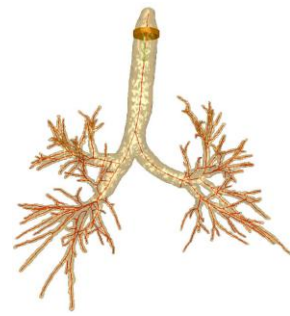


20349_3_1

N/A

N/A

1

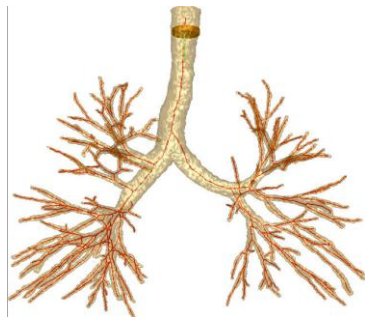


20349_3_3

N/A

N/A

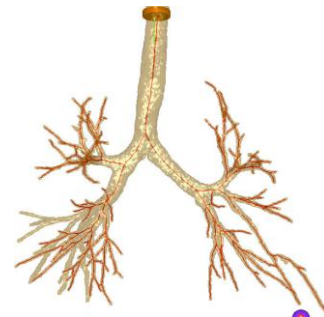
2



20349_3_6

N/A

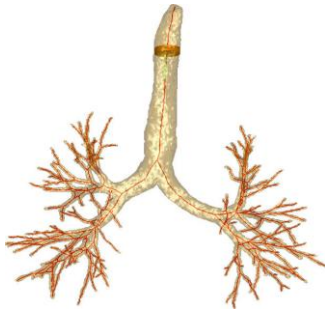
N/A



20349_3_9

N/A

N/A

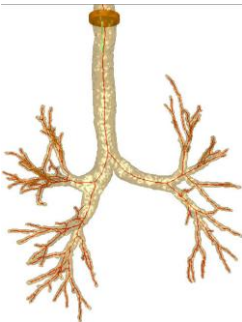


20349_3_11

N/A

N/A

2

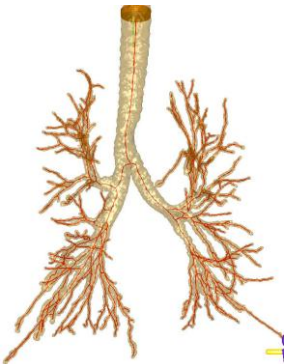


20349_3_12

N/A

N/A

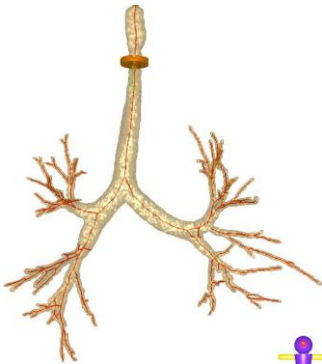
3



20349_3_13

N/A

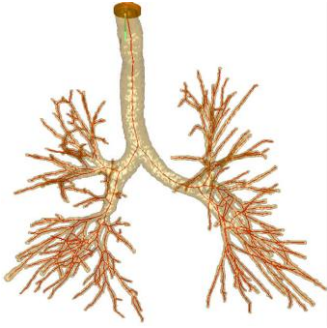
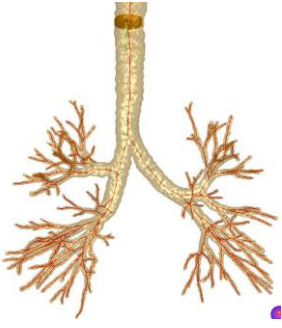
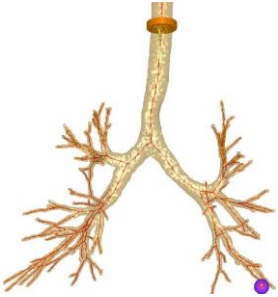
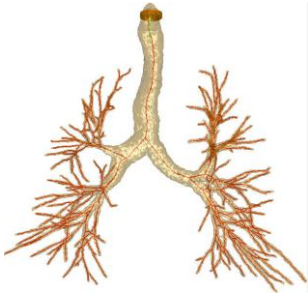
N/A

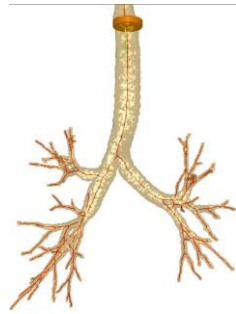


20349_3_14

N/A

N/A

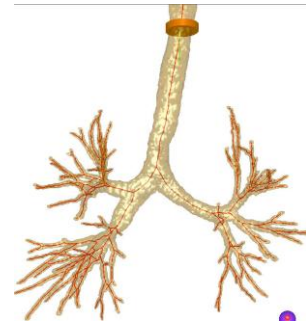
 <p>20349_3_15</p> <p>N/A</p> <p>N/A</p> <p>3</p>	 <p>20349_3_16</p> <p>N/A</p> <p>N/A</p> <p>4</p>
 <p>20349_3_17</p> <p>F</p> <p>N</p> <p>2</p>	 <p>20349_3_19</p> <p>M</p> <p>N/A</p>



20349_3_20

F

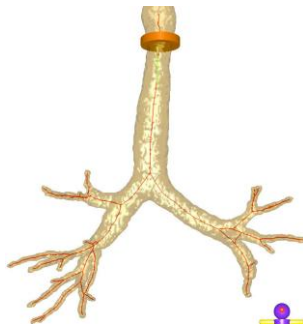
N



20349_3_21

F

Ob

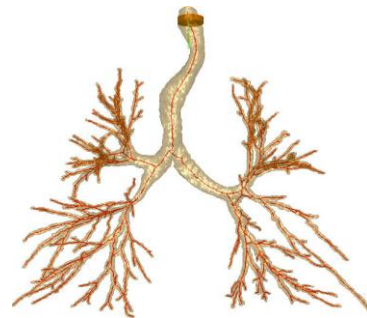


20349_3_22

F

N/A

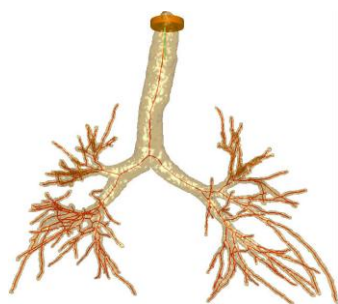
9



20349_3_23

M

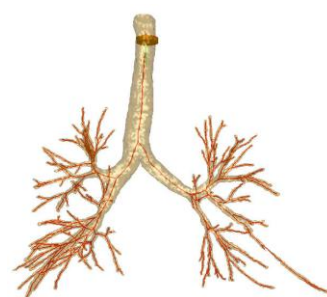
Ob



20349_3_24

F

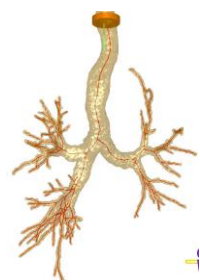
Ov



20349_3_25

M

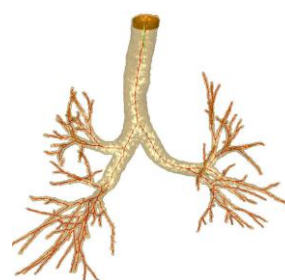
Ob



20349_3_26

F

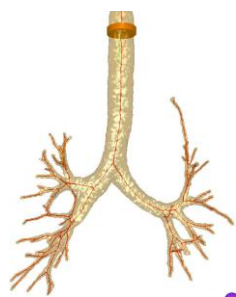
U



20349_3_27

M

Ov

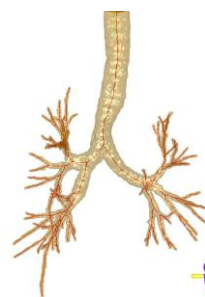


20349_3_28

F

N

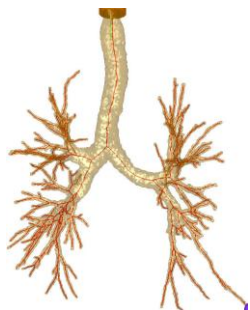
2



20349_3_29

F

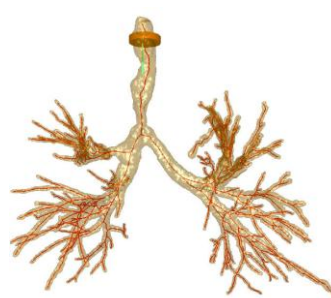
N



20349_3_30

F

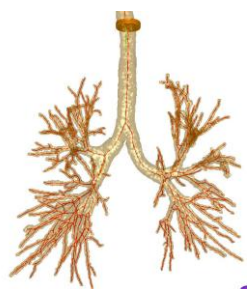
N



20349_3_31

M

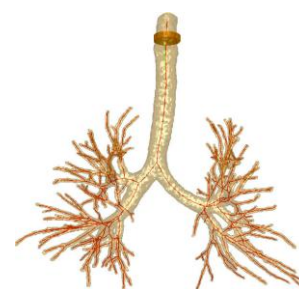
Ob



20349_3_32

F

Ov

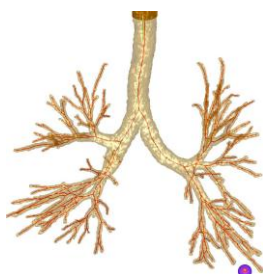


20349_3_33

M

Ov

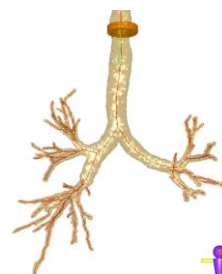
2



20349_3_34

M

Ob

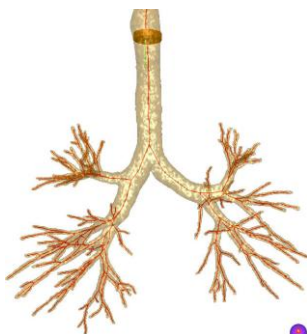


20349_3_35

F

Ob

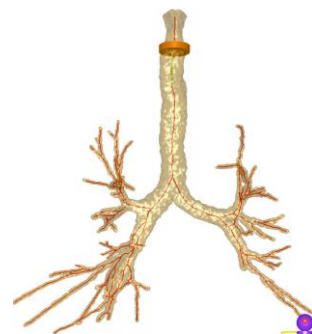
2



20349_3_36

M

Ob

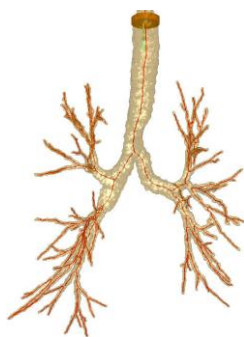


20349_3_37

F

N/A

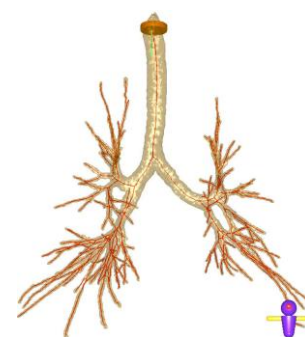
2



20349_3_38

F

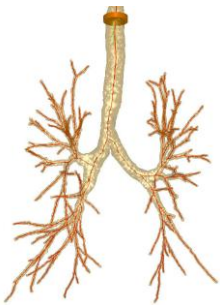
N



20349_3_39

F

N

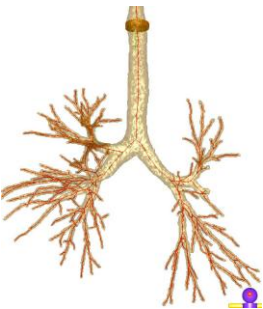


20349_3_40

F

U

5

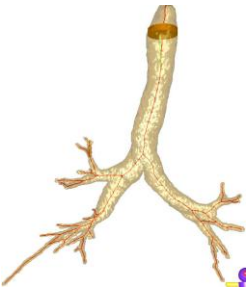


20349_3_41

F

Ob

2

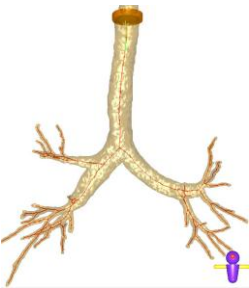


20349_3_43

M

N/A

9

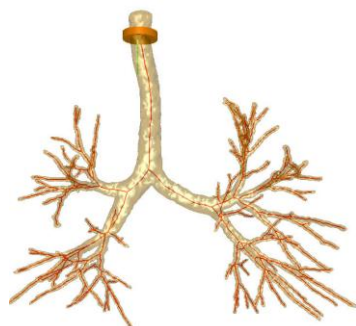


20349_3_45

M

Ob

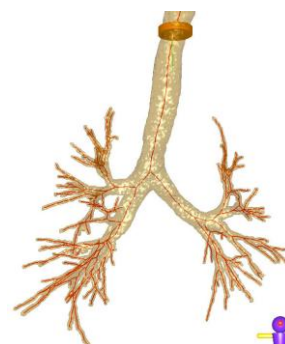
9



20349_3_46

F

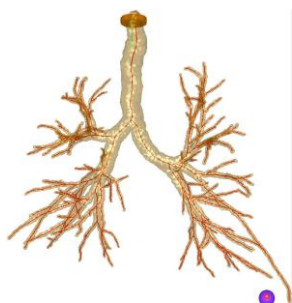
Ob



20349_3_47

F

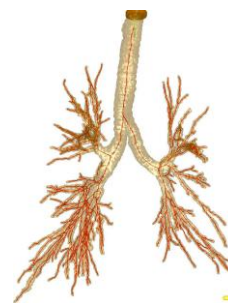
N/A



20349_3_49

M

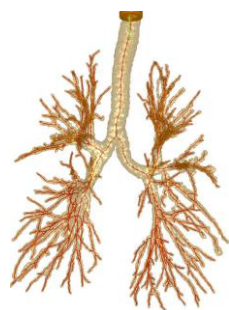
Ob



20349_3_50

F

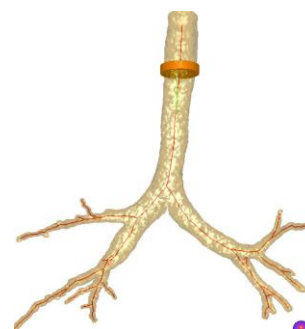
N/A



20349_3_51

F

N

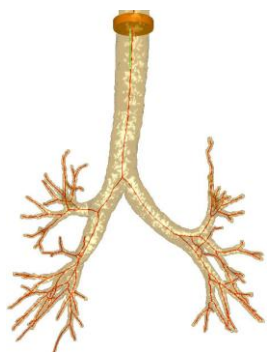


20349_3_52

F

N/A

4, 9

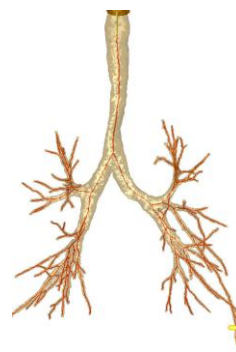


20349_3_53

F

N

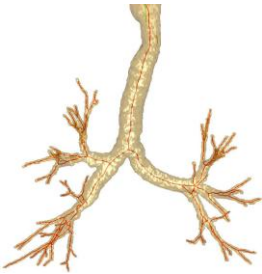
4



20349_3_55

M

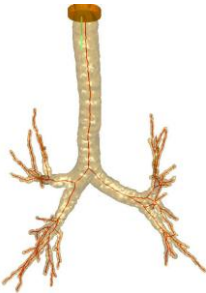
N/A



20349_3_56

M

N

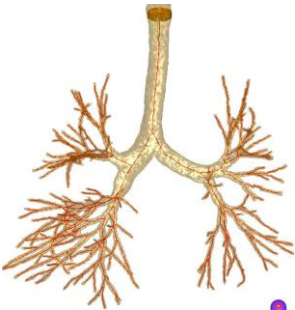


20349_3_57

F

N/A

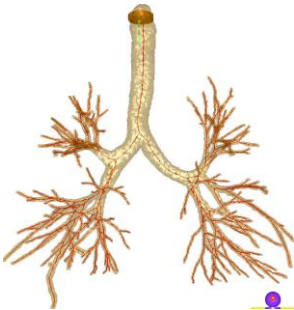
6



20349_3_58

M

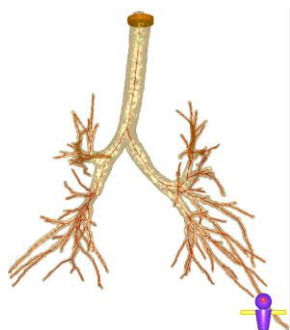
N/A



20349_3_59

M

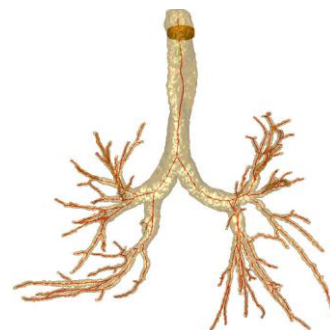
N/A



20349_3_61

F

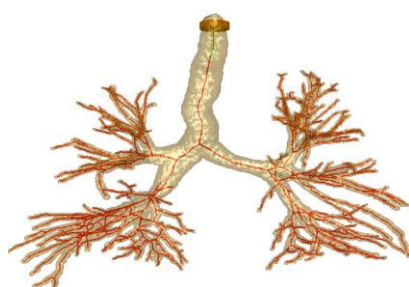
Ov



20349_3_62

M

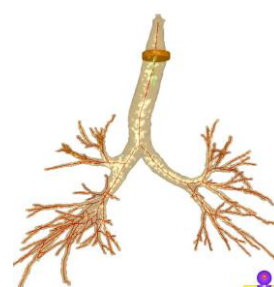
Ob



20349_3_64

M

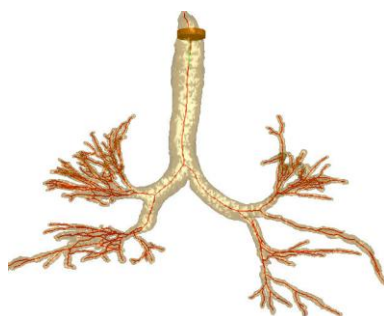
Ov



20349_3_66

F

Ov

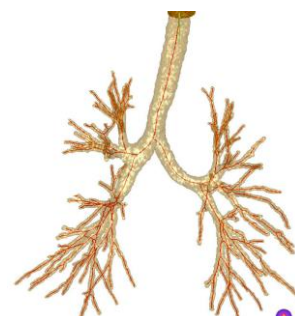


20349_3_67

M

Ob

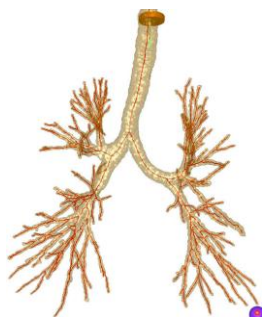
2



20349_3_68

F

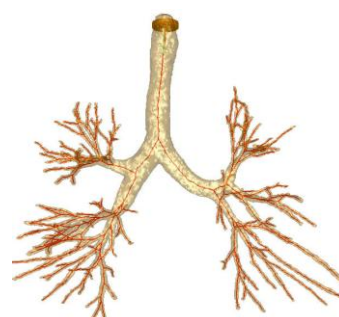
Ob



20349_3_69

F

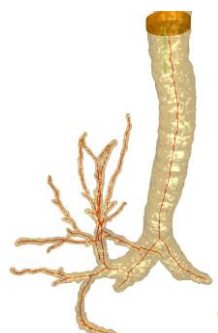
Ob



21405_12

M

Ov

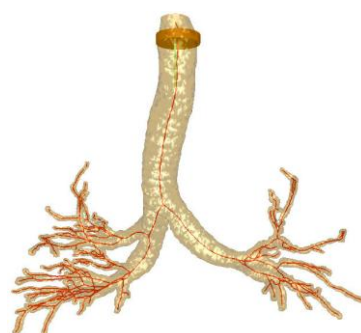


21405_19

M

Ob

9

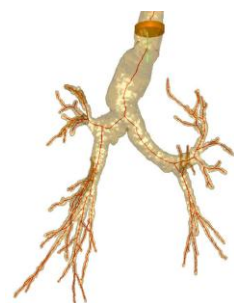


21405_20

F

U

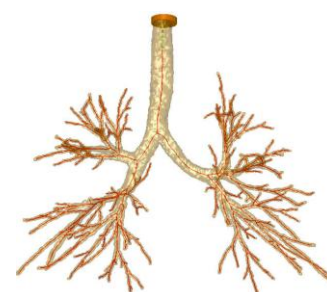
2, 7



21405_22

M

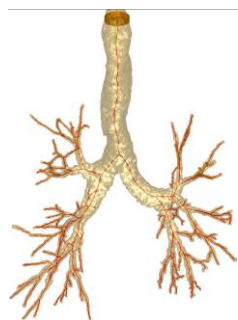
Ob



21405_57

F

Ob

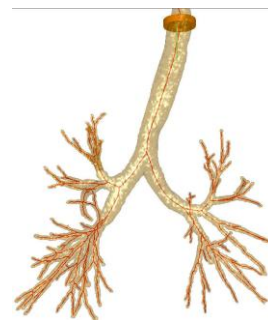


21405_59

M

N

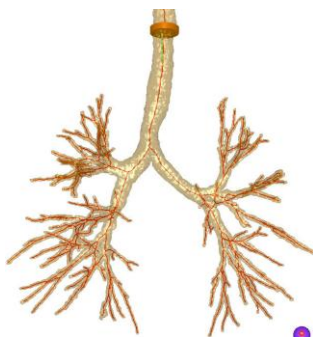
4



21405_60

F

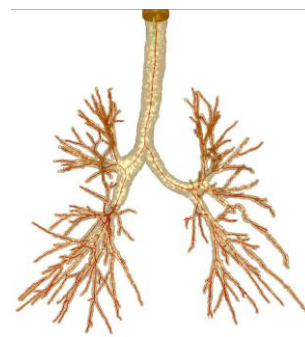
Ob



21405_63

F

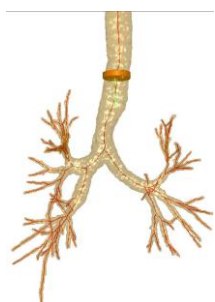
Ob



21405_64

F

Ob

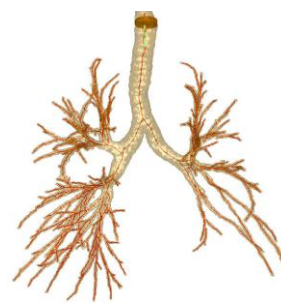


21405_66

F

N

2



21405_67

M

N

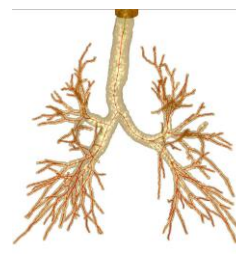


21405_69

F

N

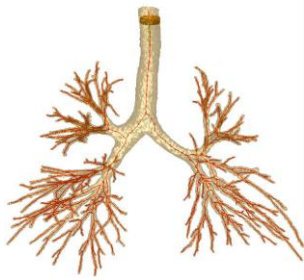
9



21405_70

F

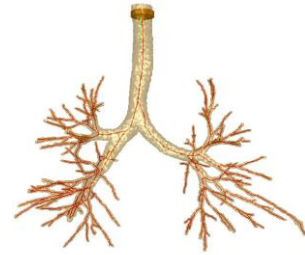
N/A



21405_72

M

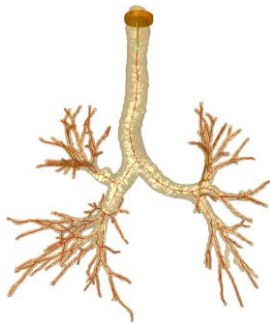
Ov



21405_73

M

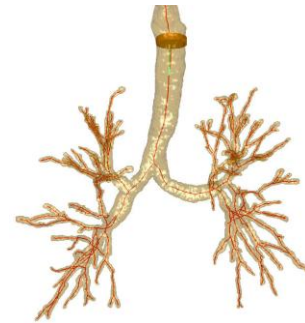
Ob



21405_74

F

Ob

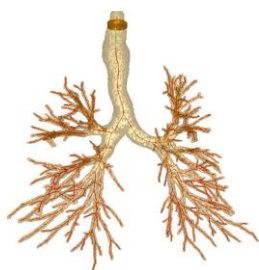


21405_75

M

N/A

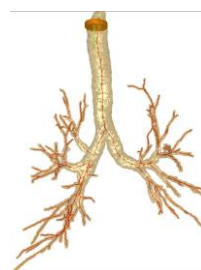
8



21405_77

M

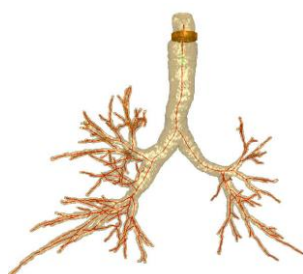
Ov



21405_78

F

N

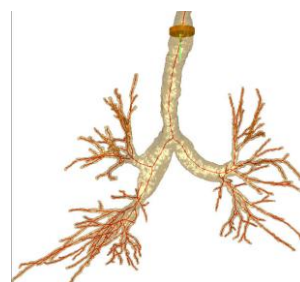


21405_80

M

Ov

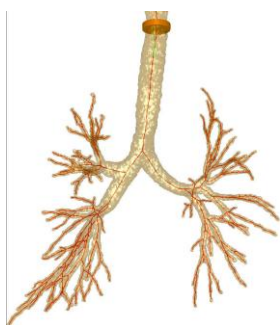
2



21405_91

M

Ov

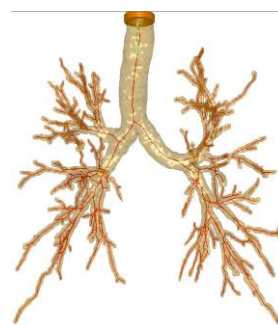


21405_92

F

N/A

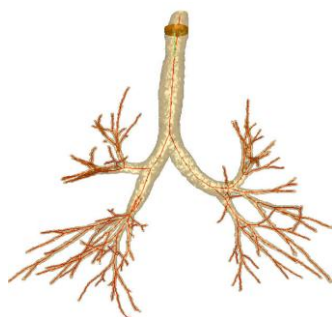
2



21405_93

F

N

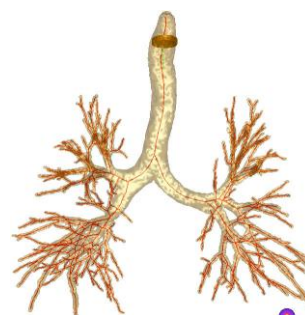


21405_95

M

Ob

4



21405_96

M

Ov

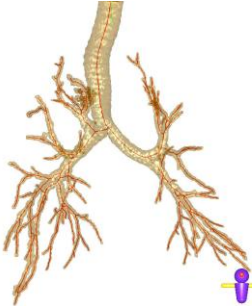
<div></div> <div>21405_97</div> <div>F</div> <div>N</div>	
--	--

Table A.2: 3D renderings of all cases used in the study. Each rendering has protocol number, gender, BMI classification, and notes corresponding to Table A.1 listed in that order underneath. M=male, F=female, U=underweight, N=normal weight, Ov=overweight, Ob=obese, and N/A=unknown.

Appendix B

User Manual

BranchStats

To generate BranchData files, we added code to the DiameterColorDialog tool developed by Duane Cornish [7]. Specifically, we added code to the file “DiameterColorDialogDlg.cpp” within the DiameterColorDialog C++ solution file.

In order to use the BranchStats program to produce a “BranchData” text file, the case must first be built. This includes segmentation, surface generation, centerline definition, and path quantitation, as described in Section 3.1. Once this is complete, the case study may be loaded into the tool and the BranchData file generated.

First, open the BranchStats tool, which may be found in the folder “\\carew\z\mra5101\MikeWork\BranchStats\x64\Release.” This will bring up a dialog box with three fields for input, labeled “Load Case Study,” “Path File,” and “Seg File,” each of which has a browse button to its right. This dialog box is shown in Figure A.1.

The first field designates which case study is to have its “BranchData” text file generated. The case study file path may be specified by first clicking on the browse button, and then by locating and selecting the case study file of interest. Upon selecting the case study file, the tool will load the case, and automatically load its associated path file, which may take several seconds. This fills in both of the first two input fields.

The third input field specifies the segmentation file to be used in computing the statistics for display. The same process should be used to select a segmentation file as was used to select a case study file; the segmentation file lies in the same folder as the case study file, as this is the default save location designated by SegTool. As such, the browse button opens the folder containing the case study selected in the first field by default, and there are generally two segmentation files available: a conservative segmentation (.cons.seg extension) and a non-conservative segmentation (.seg extension). The non-conservative segmentation is the one that should be used; the conservative segmentation is simply an intermediate file generated by SegTool.

After the case study and segmentation files have been loaded, click the “Do Calculation” button below the second input field. If the program runs successfully, a dialog box will pop up stating “Done Writing File.” The file will be saved as “BranchData.txt” and stored in the same file as the input case study file. Otherwise, the program will terminate and the text file either will not be created or will be created but not populated.

MATLAB

To perform an analysis on a particular group of text files, as detailed in section 2.3, a directory of BranchData.txt files must be organized for input to the MATLAB program. Then, both the input directory and output file destination may be specified and the program run.

In order to compile the directory of text files to be used, individual text files must be manually moved or copied into a single folder. The text files to be used depend on the desired population subgroup to be observed; for example, to perform an aggregate female analysis, identify all female cases and copy the BranchData.txt file from each case into a single folder. Because of the fact that the Branch Stats program names every text file “BranchData,” the files must be renamed upon relocation so that no two files have an identical filepath. It is highly recommended that the copied files are named according to the case study number, to ensure no ambiguity in the input directory allowing for easy removal and addition of the correct files if the desired case constituency changes.

Once the directory is created, the MATLAB program must be opened and edited to designate the input directory and output file. To do this, two programs must be opened: OverallCalc, which is the home MATLAB file and accepts the input directory, and statsTotal, which is called by OverallCalc to compute the statistics and write them to the output file. Both programs are contained in the folder

\\carew\z\mra5101\MikeWork\MATLAB. In OverallCalc, there are two lines which must be edited. The first, line 9, designates a string with which the file name is concatenated to create a full file path. For example, if the desired file identifier is

“Z\Cases\TextFiles\20349_3_50,” the “pathSet string variable should be set to ‘Z\Cases\TextFiles\’, making the full line appear as: pathSet = ‘Z\Cases\TextFiles’;.

The second line which must be altered specifies the input directory (line 15). This string will be the same as the “pathSet” string, but because it specifies a folder (rather than a string for concatenation), the final “\” character is omitted. For example, to use the directory “Z\Cases\TextFiles,” the directory should be set to ‘Z\Cases\TextFiles’. This is

done inside of the directory command in MATLAB, so the edited line will appear as: `D = dir('Z\Cases\TextFiles');`.

In `statsTotal`, there is just one line which must be edited: the desired file path of the output file (line 10). To ensure proper output file format, be sure to include the `.tab` extension on the end of the output file designation. For example, if the file is to be saved as `"Z\Compilation Files\Analysis.tab"`, the line should appear as `"fidwrite = fopen('Z\Compilation Files\Analysis.tab', 'w');"`. Once these three lines are specified, the program is ready to generate the desired output file.

When the program is run, it will create the output file with the designated name in the specified location. This `.tab` file may then be opened directly in Microsoft Excel, and any desired data may be manipulated in Excel to form charts, tables, and any other display formats necessary for further understanding.

BIBLIOGRAPHY

- 1] Ewald R. Weibel, *Morphometry of the Human Lung*, Berlin: Springer-Verlag, 1963.
- 2] Henry N. Wagner, "The Lungs," in *The Johns Hopkins Atlas of Functional Human Anatomy*, Baltimore: The Johns Hopkins University Press, 1997, pp. 114-117.
- 3] Willi Kalender, *Computed Tomography: Fundamentals, System Technology, Image Quality Applications*, Bavaria: Erlangen, 2011.
- 4] A. William Sheel, Jordan A. Guenette, Ren Yuan, Lukas Holy, John R. Mayo, Annette M. McWilliams, Stephen Lam and Harvey O. Coxson, "Evidence for dysanapsis using computed tomographic imaging of the airways in older ex-smokers," *Journal of Applied Physiology*, no. 107, pp. 1622-1628, 2009.
- 5] Merryn H. Tawhai, Peter Hunter, Juerg Tschirren, Joseph Reinhardt, Geoffrey McLennan and Eric A. Hoffman, "CT-based geometry analysis and finite element models of the human and ovine bronchial tree," *Journal of Applied Physiology*, no. 97, pp. 2310-2321, 2004.
- 6] Michael W. Graham, Jason D. Gibbs, Duane C. Cornish and William E. Higgins, "Robust 3-D Airway Tree Segmentation for Image-Guided Peripheral Bronchoscopy," *IEEE Transactions*

on Medical Imaging, vol. 29, no. 4, pp. 982-997, 2010.

- 7] William E. Higgins, Jason D. Gibbs, Lav Rai, Michael W. Graham, Kun-Chang Yu, Rahul Khare, Brett Flood, Kongkuo Lu, Tony Sherbondy, Allen Austin, Jim Helferty and David Zhang, *Off-line Tools for the Virtual Navigator System*, Departments of Electrical Engineering, CSE, and Bioengineering, The Pennsylvania State University, State College, Pennsylvania, 2012.
- 8] Neal C. Dalrymple, Srinivasa R. Prasad, Michael W. Freckleton and Kedar N. Chintapalli, "Introduction to the Language of Three-dimensional Imaging with Multidetector CT," *RadioGraphics*, vol. 25, no. 5, pp. 1409-1428, 2005.
- 9] "BMI classification," World Health Organization, 12 4 2013. [Online]. Available: http://apps.who.int/bmi/index.jsp?introPage=intro_3.html. [Accessed 12 4 2013].
- 10] Scott A. Merritt, Jason D. Gibbs, Kun-Chang Yu, Viral Patel, Lav Rai, Duane Cornish, Rebecca Bascom and William E. Higgins, "Image-Guided Bronchoscopy for Peripheral Lung Lesions: A Phantom Study," *Chest*, vol. 134, no. 5, pp. 1017-1026, 2008.
- 11] William E. Higgins, James P. Helferty, Kongkuo Lu, Scott A. Merritt, Lav Rai and Kun-Chang Yu, "3D CT-Video Fusion for Image-Guided Bronchoscopy," *Computerized Medical Imaging and Graphics*, vol. 32, pp. 159-173, 2008.

- 12] Jason D. Gibbs, Michael W. Graham and William E. Higgins, "3D MDCT-based system for planning peripheral bronchoscopic procedures," *Computers in Biology and Medicine*, vol. 39, pp. 266-279, 2009.
- 13] A.P. Kiraly, James P. Helferty, E.A. Hoffman, G. McLennan and William E. Higgins, "Three-Dimensional Path Planning for Virtual Bronchoscopy," *IEEE Transactions on Medical Imaging*, vol. 23, no. 9, pp. 1365-1379, 2004.
- 14] Junji Ueno, Tomoya Murase, Kazuhide Yoneda, Tetsuya Tsujkawa, Shoji Sakiyama and Kazuya Kondoh, "Three-dimensional imaging of thoracic diseases with multi-detector row CT," *The Journal of Medical Investigation*, vol. 51, pp. 163-170, 2004.

ACADEMIC VITA

Michael Amthor

1311 Fenwick Drive

Harrisburg, Pa 17110

mamthor5101@gmail.com

Education

B.S., Electrical Engineering, 2013, The Pennsylvania State University, University Park,
Pennsylvania

Honors and Awards

- Phi Mu Delta Charles S. Rising Outstanding Chapter President Award, Phi Mu Delta National Fraternity - 2012
- William J. Madden and Ethel Harer Madden Memorial Scholarship in Engineering, The Pennsylvania State University - 2010, 2011, 2012
- President's Freshman Award, The Pennsylvania State University - 2011
- Dean's List, The Pennsylvania State University - Semesters Spring & Fall 2010, Spring & Fall 2011, Fall 2012
- Dean's List, The University of Alabama – Semester Fall 2009
- National Merit Scholar - National Merit Scholarship Corporation - 2009

Association Memberships/Activities

- Phi Mu Delta Fraternity
- Eta Kappa Nu Electrical Engineering Honor Society

Professional Experience

- Hershey Medical Center: Medical Imaging Research Intern (Summer 2012) Worked under Dr. William Higgins on 3D-reconstruction of the human airway tree from high resolution CT images. Assisted with the navigation and recording of four bronchoscopy procedures including planning, execution, and documentation. Also assisted with writing procedural protocol as well as lab operations and upkeep.

- Z-Band Video: Electrical Engineering Intern (May 2011 - January 2012) Performed product integrity testing for both current product units and future product prototypes in addition to fixing broken units over summer and winter breaks. This included frequent use of a spectrum analyzer for comparing output frequency spectra to known standards as well as reorganizing engineering documentation.